Article

Temozolomide, Simvastatin and Acetylshikonin Combination Induces Mitochondrial Dependent Apoptosis in GBM Cells which is Regulated by Autophagy

Sima Hajiahmadi[1], Shahrokh Lorzadeh[2], Rosa Iranpour[2], Saeed Karima[1], Masoumeh Rajabibazl[1], Zahra Shahsavari[1] and Saeid Ghavami[2,3,4*]

1 Department of Clinical Biochemistry, Faculty of Medicine, Shahid Beheshti University of Medical Sciences, Tehran, Iran
2 Department of Human Anatomy and Cell Science, Max Rady College of Medicine, University of Manitoba, Winnipeg, MB R3E 0V9, Canada
3 Faculty of Medicine in Zabrze, Academia of Silesia, 41-800 Zabrze, Poland
4 Research Institute of Oncology and Hematology, Cancer Care Manitoba, University of Manitoba, Winnipeg, MB R3T 2N2, Canada
*Corresponding: Dr. Saeid Ghavami, Associate Professor, Department of Human Anatomy and Cell Science, Max Rady College of Medicine, University of Manitoba, Winnipeg, MB R3E 0V9, Canada, Email: saeid.ghavami@umanitoba.ca

Simple Summary: Glioblastoma Multiforme (GBM) is a deadly brain tumor. The current chemotherapy strategies [including using the Temozolomide (TMZ)] is not very effective for GBM patients. Therefore, finding a new therapeutic strategy is demanding in the field of GBM. In our current investigations, we used an innovative combination of TMZ, and FDA-approved cholesterol lowering medication (simvastatin), and a Chinese herbal medicine derivative [Acetylshikonin (ASH)] in GBM cell lines. Our investigation showed that the triple combination treatment (TMZ/Simva/ASH) induced significant more cell death via damaging the energy engine of the cells (mitochondria). In addition, inhibition of the cellular self-eating mechanism (autophagy) sensitize the GBM to triple combination-induced cell death. Overall, the current research may open new avenue in treatment of GBM patients in the long term.

Abstract: Glioblastoma multiforme (GBM) is one of the deadliest cancers. Temozolomide (TMZ) is the most common chemotherapy used for GBM patients. Recently, combination chemotherapy strategies have more effective antitumor effects and focus on slowing down the development of chemotherapy resistance. A combination of TMZ and cholesterol lowering medications (statins) is currently under investigation in *in vivo* and clinical trials. In our current investigation, we have used a triple combination therapy of TMZ, Simvastatin (Simva), and Acetylshikonin (ASH) and investigated its apoptotic mechanism in GBM cell lines (U87 and U251). We used viability, apoptosis, reactive oxygen species (ROS), mitochondrial membrane potential (MMP), caspase-3/-7, acridine orange (AO) and immunoblotting autophagy assays. Our results showed that TMZ/Simva/ASH combination therapy significantly induced more apoptosis compared to TMZ, Simva, ASH, and TMZ/Simva treatments in GBM cells. Apoptosis via TMZ/Simva/ASH treatment induced mitochondrial damage (increase of ROS, decrease of MMP) and induced caspase-3/7 activation in both GBM cell lines. Compared to all single treatments and the TMZ/Simva treatment, TMZ/Simva/ASH significantly increased positive acidic vacuole organelles. We further confirmed that the increase of AVOs during the TMZ/Simva/ASH treatment was due to partial inhibition of autophagy flux (accumulation of LC3β-II and decrease in p62 degradation) in GBM cells. Our investigation also showed that TMZ/Simva/ASH-induced cell death was depended on autophagy flux as further inhibition of autophagy flux increased TMZ/Simva/ASH-induced cell death in GBM cells. Finally, our results showed that TMZ/Simva/ASH treatment potentially depends on an increase of Bax expression in GBM cells. Our current investigation might open new avenues for more effective treatment of GBM but further investigations are required for better identification of the mechanisms.

 doi:10.20944/preprints202301.0247.v1

Keywords: statin; natural compounds; Bcl2 family proteins; intrinsic apoptosis pathway; caspase dependent apoptosis

1. Introduction

Among the known adult malignant brain tumors, glioblastoma multiforme (GBM) is the most aggressive glioma [1]. Despite advances in medical technologies, the average life-span of GBM patients after surgery and chemotherapy is 14-15 months [2]. Although the annual incidence rate of GBM is about 3.19 to 4.17 cases per 100,000 people [3], its high mortality rate and poor prognosis encourage researchers to find more effective treatments [4].

TMZ is widely used as the first line of chemotherapy for GBM patients [5,6]. It is an alkylating agent [7,8] and induces DNA damage, cell cycle arrest and apoptosis activation [8-10]. TMZ also induces autophagy which could have cytoprotective effects on the target cells [9-11].

The cell fate is determined via different mechanisms including apoptosis, autophagy, and the unfolded protein response (UPR) [12,13]. These pathways are initiated and characterized by multiple stimuli and signaling mediators [14,15]. The main function of autophagy relates to the cell's protection and survival, while under some situations it leads to cell death [16,17]. There are different molecular pathways for crosstalk between the apoptosis and autophagy pathways [18-20]. Autophagy can be a pro- or anti-apoptotic mechanism based on the type of cell model, organism and the stimuli [21-24].

Statins are cholesterol lowering drugs with several pleiotropic effects including their impact on cancer [25]. In recent years, both basic and clinical scientists have focused their investigations on the potential role of statins in cancer therapy. Recent studies have suggested that statins could have beneficial effects and impacts on the response to chemotherapy in cancer patients [9,26-29]. A recent investigation has showed that simvastatin combined with TMZ increases the survival of GBM patients [30]. Our team has recently discovered that simvastatin induces apoptotic cell death in glioblastoma, non-small cell lung carcinoma, breast cancer, and neuroblastoma cell lines via depletion of geranylgernaly pyrophosphate [31,32]. We have later showed that simvastatin sensitizes GBM tumor cell lines (U87, and U251) and primary patient derived GBM cells to TMZ-induced apoptosis via inhibition of autophagy flux [33] and UPR [20].

Recently, Shikonin (SHK) [32], a highly lipophilic compound from Lithospermum erythrorhizon root that is commonly used in Chinese folklore remedies through its anti-inflammatory and pleiotropic effects, has been introduced as an antitumor agent [34-38]. Besides the strong anticancer feature of Shikonin and its analogs, they also have the ability of circumventing cancer drug resistance [39,40]. Shikonin derivatives like Acetylshikonin (ASH) have shown cytotoxic and anti-cancer effects [41]. A few recent investigations also showed the impact of SHK (alone or in combination with TMZ) in targeting GBM tumor cells by inducing significant apoptotic cell death and decreasing their proliferation [42,43].

In the current investigation, we expand our previous investigations and used triple treatments of ASH, TMZ and Simvastatin (Simva) to target GBM tumor cells (U251 and U87). We focused our investigation on the mechanism of combination therapy on GBM cells via cross talk of apoptosis and autophagy.

2. Materials and Methods

2.1. Reagents and Drugs

Acetylshikonin (CAS Number: 24502-78-1) and simvastatin (CAS Number: 79902-63-9) were purchased from Chem Face China Company. Temozolomide (CAS Number: 85622-93-1), propidium iodide (CAS Number: 25535-16-4), 3-[4,5-dimethylthiazol-2-yl]-2,5 diphenyl tetrazolium bromide (MTT) (CAS Number: 298-93-1), Acridine Orange (CAS Number: 65-61-2), Bafilomycin A1(Cat#: B1793-10UG) and anti-rabbit LC3β antibody

 doi:10.20944/preprints202301.0247.v1

(Cat# L7543-100UL) were purchased from Sigma-Aldrich Co. Anti-rabbit p62 antibody (Cat#39749), anti-rabbit Beclin-1 antibody (Cat#3738), anti-mouse Bcl2 antibody (Cat#15071), anti-rabbit Mcl-1 antibody (Cat#4572), anti-rabbit Bcl-XL antibody (Cat#2762), and anti-rabbit GAPDH antibody (Cat#2118) were purchased from Cell Signaling Company. The secondary antibodies, anti-rabbit HRP-conjugate and anti-mouse HRP-conjugate were purchased from Sigma-Aldrich (Oakville, ON, Canada) as well. The enhanced chemiluminescence (ECL) (CAS Number: 12630) was acquired from Cell Signaling Technology Co. (Beverly, MA, USA). The bicinchoninic acid (BCA) protein assay kit was obtained from Thermo Fisher Scientific (Winnipeg, MB, Canada).

2.2. Cell Lines, Culture, and Treatment

U87 and U251 human GBM cells were obtained from Bon yakhteh Company (Bon yakhteh, Tehran, Iran) and cultured in Dulbecco's Modified Eagle's Medium (DMEM) (Bio Idea, Tehran, Iran, Cat #: DB9696) (low-glucose, high glutamine for U87 and high-glucose for U251), supplemented with 10% Fetal Bovine Serum (FBS) (Bio Idea, Tehran, Iran, Cat #: BI-1201) and 1% penicillin–streptomycin (Bio Idea, Tehran, Iran, Cat #: BI-1203). Cells were maintained in a 5% CO2 incubator with 95% humidity at 37 °C.

2.3. Cytotoxicity Assay

To evaluate the cytotoxicity effects of Temozolomide, ASH and Simva and their combination on U87 and U251 GBM cell lines, MTT viability tests were done based on our established method [8,24,31-33,44]. Four different time points (24, 48, 72 and 96 hrs) and a range of concentrations (TMZ 50-250 μM, ASH 0.5-25 μM, Simva 0.5-20 μM) were tested. After finding the best time point and the IC50 concentration of each drug, the combination therapy of TMZ/Simva and TMZ/Simva/ASH on GBM cells was evaluated. For combination therapy, Simva was pretreated for 4 hrs. U87 and U251 cells were both briefly cultured in 96-well plates (6000 cells per well) and treated with different concentrations of the drugs. After the treatment time point, 20 μL of MTT dye, 3-[4,5-dimethylthiazol-2-yl]-2,5 diphenyl tetrazolium bromide was added to each well and incubated in the 37 °C incubator for 4 h. The medium was then aspirated and 200 μL of DMSO was added to each well and incubated at room temperature for 15 min in the dark. Finally, the optical absorbance was read at 570 nm by multiplate reader (Synergy, Biotek, USA).

2.4. Apoptosis Assay Using Flow Cytometry

The cell death mechanism evaluation was measured using Nicolleti method [45-49]. Both cell lines were briefly cultured in 6-well plates (100,000 cells per well) and pre-treated with Simva 1 μM and 2.5 μM for U251 and U87 respectively, for 4 hrs. These were the least toxic concentrations of Simva for each cell line. Then, TMZ 100 μM and ASH 1.5 μM were added. After 72 hrs, the cells were detached by EDTA buffer to minimize cell damage and then washed with PBS. Afterward, PI lysis buffer including 0.1% Triton X-100, 40 μg/mL propidium iodide, 1% sodium citrate and 0.5 mg/mL RNase A were added to the obtained pellets and incubated at 37 °C for 35 min. Finally, sub G1 population area indicated the apoptotic nuclei levels by Flow Cytometry (FACScalibur flow cytometer, BD Biosciences, USA). All the results were acquired in 10,000 event count.

2.5. Immunoblotting

We did western blotting according to our previous investigations [44,50-52]. After treatment with the different compounds [TMZ-Simva-ASH, ASH, Bafilomycin A1 (Baf-A1)] at the indicated time point (72 hrs), the cells were gently washed with PBS, and the pellets were collected. The pellets were suspended in lysis buffer including NaCl 150 Mm, Triton 1%, Tris 50 Mm, protease inhibitor and Phosphatase inhibitor cocktail (Cat# P5726-Sigma) and then sonicated 5 times for 3 seconds. Equal amounts of proteins were loaded onto the electrophoresis SDS-PAGE gel. The proteins were then transferred to PVDF membranes (Sigma; # IPVH00010). The blocking step was performed in 5% fat-free milk

 doi:10.20944/preprints202301.0247.v1

overnight. The primary antibodies (Bax, Bcl-2, LC3β-II and p62) were also diluted based on the manufacture's protocol to add the membranes and incubate at 4 °C overnight. The next step was the incubation of the membranes with corresponding secondary antibodies at room temperature for 90 min. Finally, the membranes were exposed to enhanced chemiluminescence (ECL) reagents and developed by the ChemiDocTM MP imaging system (Bio-Rad, Hercules, CA, USA). To quantify the intensity of the bands, Image Lab densitometry software was utilized and normalized by GAPDH protein values to correct the possible errors during protein loading.

2.6. Caspase3/7 activation assay

To assess the activity and catalytic function of caspase3/7 (DEVD-ase), Cayman fluorescence assay kit was used based on our adopted established protocol [31,33,46]. Briefly, the cells were seeded in 96 wells plates to reach about 50% confluence to prevent high non-specific fluorescence, and were then treated with TMZ (100 μM), Simva (1 and 2.5 μM for U251 and U87 respectively), ASH (1.5 μM), TMZ/Simva and TMZ/Simva/ASH for 48 hrs based on our experimental protocol (OEP). For the combinations, Simva was pretreated for 4 h. All reagents were freshly prepared including assay buffer, caspase3/7 substrate, active caspase-3 positive control and caspase3/7 inhibitor solution. The plates were centrifuged at 800 g for 5 min, followed by aspiration of the supernatant, addition of assay buffer and another centrifugation. Later, lysis buffer was added, followed by orbital shaking and centrifuging (800 g). Caspase3/7 inhibitor, active caspase-3 positive control and caspase3/7 substrate solutions were then added (30 min, room temperature, and dark place). The fluorescence intensity of each well was measured by BioTek Cytation 3 Cell Imaging MultiMode Microplate Reader (Biotek Cytation 3, USA) (excitation wavelength: 485 nm, emission wavelength: 535 nm).

2.7. Reactive Oxygen (ROS) Assay

ROS generation was detected by Cayman ROS detection cell based Dihydroethidium (Hydroethidine, DHE) assay. The cells were cultured in the black tissue culture-treated 96-well plates, where their confluence reached about 70% after 24 hrs to avoid overgrown cells. The treatment was done at two different point times (38, 60 h). The cell-based assay buffer and DHE, N-Acetyl cysteine and Antimycin assay reagents were prepared based on the kit protocol. All wells were aspirated. The assay buffer and ROS staining buffer were then added respectively. N-Acetyl cysteine and Antimycin were used as the negative and positive controls, respectively. The kit's instruction was followed for the incubation times, fluorescence was measured (excitation wavelength of 480-520 nm and emission wavelength of 570-620 nm) and microscopic images were taken by BioTek Cytation 3 Cell Imaging MultiMode Microplate Reader (Biotek Cytation 3, USA) and analyzed based on our established protocols [33].

2.8. Determination of Mitochondria Membrane Potential (MMP)

Loss of mitochondria membrane potential is considered a substantial parameter of cell function. Thus, the measurement of changes in MMP is very important to follow the apoptotic process. After seeding the cells in the 96-well black culture plates and treatment for 48 hrs, Cayman JC-1 mitochondria membrane potential assay kit was used. The cells' confluence was 80% at the time of staining. JC-1 was added to each well and the assay buffer was used after incubation. The test was performed based on the kit directions. The healthy cells with JC-1 J-aggregates were detected with Rhodamine filter (excitation/emission: 540/570) while the apoptotic cells with mainly JC-1 monomers were detectable with FITC filter (excitation/emission 485/540) by BioTek Cytation 3 Cell Imaging MultiMode Microplate Reader (Biotek Cytation 3, USA).

 doi:10.20944/preprints202301.0247.v1

2.9. Acridine Orange Acidic Vacuole Assay

To detect the acidic vesicular organelles [53], which are essential markers of late autophagy [54], acridine orange (AO) staining assay was performed. AO induces green fluorescence in cytosolic and nuclear parts of the cells, but upon fusion into the acidic environment such as lysosomes, it becomes protonated and emits an intense red fluorescence. So, the ratio of red to green fluorescence intensity can be a suitable marker for AVO formation. Cells were seeded at 96-well plates and treated for 72 hrs. They then were stained with AO (final concentration of 1 μg/mL) and incubated at 37 °C for 10 minutes (dark and room temperature). After washing with PBS twice, the microscopic images were taken and the green and red fluorescence was read at 550 and 650 nm of emission wavelengths by BioTek Cytation 3 Cell Imaging MultiMode Microplate Reader (Biotek Cytation 3, USA), respectively.

2.10. Statistical Analysis

The results were represented as means ± SD and statistical differences were analyzed by one-way or two-way ANOVA using Graph Pad Prism 8. *P*-value < 0.05 implies the significance values. All the experiments were done in at least three biological replicates.

3. Results

3.1. TMZ/Simva/ASH Combination Treatment Induces More Cell Death Compared to Single Treatment in Human GBM Cells.

Our previous investigations have showed that co-treatment of Simva/TMZ increased cytotoxicity effects in comparison to TMZ and Simva single treatment in GBM cells (U251 and U87) [10,55]. ASH was used in combination with Simva/TMZ in our current investigation, as it induces cell death in different tumor models, including GBM cells, [56-58] and crosses the blood brain barrier [58]. We investigated if this combination induces more cell death compared to the single therapies and the Simva/TMZ combination therapy.

Initially we determined the cytotoxic effects of ASH, TMZ, and Simva in U251 and U87 cells. We treated these cells with different concentrations of ASH, TMZ, and Simva [ASH (0.5-25 μM), TMZ (50-250 μM), and Simva (0.5-20 μM)] at different time points (24, 48, 72 and 96 h). Our results showed that all concentrations of Simva induced significant cell death ($P<0.0001$) except 0.5 μM at 24 and 48h hrs ($P>0.05$) in U251 (Figure 1 A-D) and U87 (Supplementary Figure 1 A-D) cells. We also determined that all concentrations of TMZ induced significant cell death ($P<0.0001$, $P<0.05$) in U251 (Figure 1 E-H) and U87 (Supplementary Figure 1 E-H) cells, except for 50 μM at 24 and 48h hrs ($P>0.05$). Our investigations also showed that all concentrations of ASH induced significant cell death ($P<0.0001$, $P< 0.05$, $P<0.01$) in U251 (Figure 1 I-L) and U87 (Supplementary Figure 1 I-L) cells. 0.5 μM concentration of ASH did not induce significant cell death at 24 hrs in U87 cells.

In the next step we identified the cytotoxic effects of Simva/TMZ/ASH in GBM cells. Based on our previous investigations [20,33] and results of single treatments, we used Simva (1 μM, U251; and 2.5 μM, U87), TMZ (100 μM) and ASH (1.5 μM) for 72 hrs based on the minimum toxic dose (<25%). Our findings showed that TMZ/Simva/ASH combination therapy induced significantly higher cell death compared to single therapies (TMZ, Simva, ASH) in both U251 (Figure 2 A-D) and U87 (Supplementary Figure 2 A-D) at 72 hrs ($P<0.0001$). Furthermore, the results showed that ASH significantly increased the toxicity effects of TMZ/Simva in both U251 and U87 cells at 72 hrs ($P<0.0001$), (Figure 2 A-D, Supplementary Figure 2 A-D).

Preprints (www.preprints.org) | NOT PEER-REVIEWED | Posted: 13 January 2023 doi:10.20944/preprints202301.0247.v1

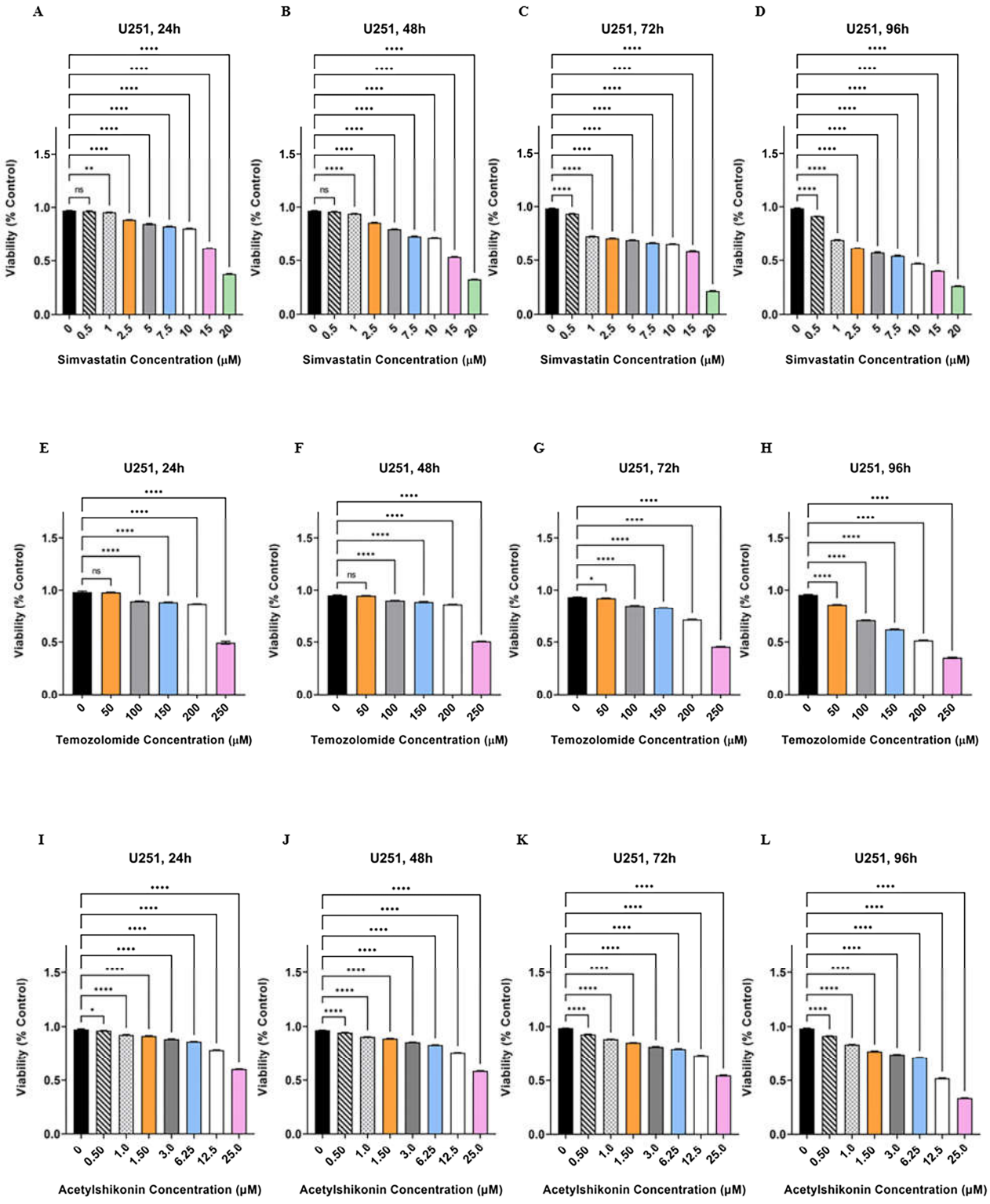

Figure 1. Simvastatin, Temozolomide and Acetylshikonin induce cell death in human glioblastoma cells. U251 cells were treated with different concentrations of Simva (0.5-20μM, **A-D**), TMZ (50-100 μM, **E-H**), and ASH (0.5-25 μM, **I-L**) at four time points (24, 48, 72 and 96 hrs). The cytotoxicity of each treatment was measured using MTT assay. The percentage of cell viability was measured (*ns*= non-significant; *=*P*<0.05; **=*P*<0.01; ****=*P*<0.0001) compared to time match vehicle control. Simva induced significant decrease in cell viability (*P*<0.0001) for all concentrations at all time points except 0.5 μM at 24 and 48 hrs (*P*>0.05) and 1 μM at 24 hrs (*P*<0.01). TMZ induced significant cell death

 doi:10.20944/preprints202301.0247.v1

(P<0.0001) for all concentrations at all time points except 50 μM at 24 and 48 hrs (P>0.05) and 50 μM at 72 hrs (P<0.05). ASH induced significant cell death (P<0.0001) for all concentrations at all time points except 0.5 μM at 24 hrs (P<0.05). The represented findings are from 9 replicates in three independent biological assays and showed as mean ±SD.

3.2. TMZ, Simva, ASH, TMZ/Simva and TMZ/Simva/ASH Treatments Induce Caspase-Dependent Apoptosis in GBM Cells.

In our study, we used TMZ, Simva, ASH, TMZ/Simva and TMZ/Simva/ASH treatments to induce apoptosis in GBM cells. Concentrations of 1 μM Simva for U251, 2.5 μM Simva for U87, 100 μM TMZ (U251 and U87), and 1.5 μM ASH (U251 and U87) were used. The results showed that the apoptotic cell population for TMZ/Simva was 21 and 24% in U87 and U251, respectively, which is significantly higher than for TMZ (12%) and Simva (6%) single treatments in both cells at 72 hrs (P<0.0001) (Figure 2E). TMZ/Simva/ASH combination significantly increased apoptosis compared to TMZ/Simva and ASH single therapy in U87 and U251 cells (P<0.0001), (Figure 2 F-G).

Caspase-3/-7 are the final executing caspases and induce the last steps in nuclear events related to apoptosis [38,59,60]. We measured their activity at 60 hrs to investigate the impact of Caspase activation in TMZ, Simva, ASH, TMZ/Simva, and TMZ/Simva/ASH-induced apoptosis in GBM cells. Our results showed that Caspase-3/-7 was significantly activated in all treatment conditions in U87 (Figure 2H) and U251 (Figure 2I) cells (P<0.0001). Our results also showed that TMZ/Simva and TMZ/Simva/ASH combination therapy showed higher significant Caspase-3/-7 activation in both cell lines compared to single treatment (P<0.0001) (Figure 2H-I). Additionally, the TMZ/Simva/ASH combination treatment induced significantly higher activation of Caspase-3/-7 compared to TMZ/Simva treatment in both U87 and U251 cells (P<0.0001) (Figure 2H-I). These findings correlated with higher apoptosis induction in triple combination treatments for both cell lines compared to TMZ/Simva treatment (P<0.0001) (Figure 2H-I).

Preprints (www.preprints.org) | NOT PEER-REVIEWED | Posted: 13 January 2023 doi:10.20944/preprints202301.0247.v1

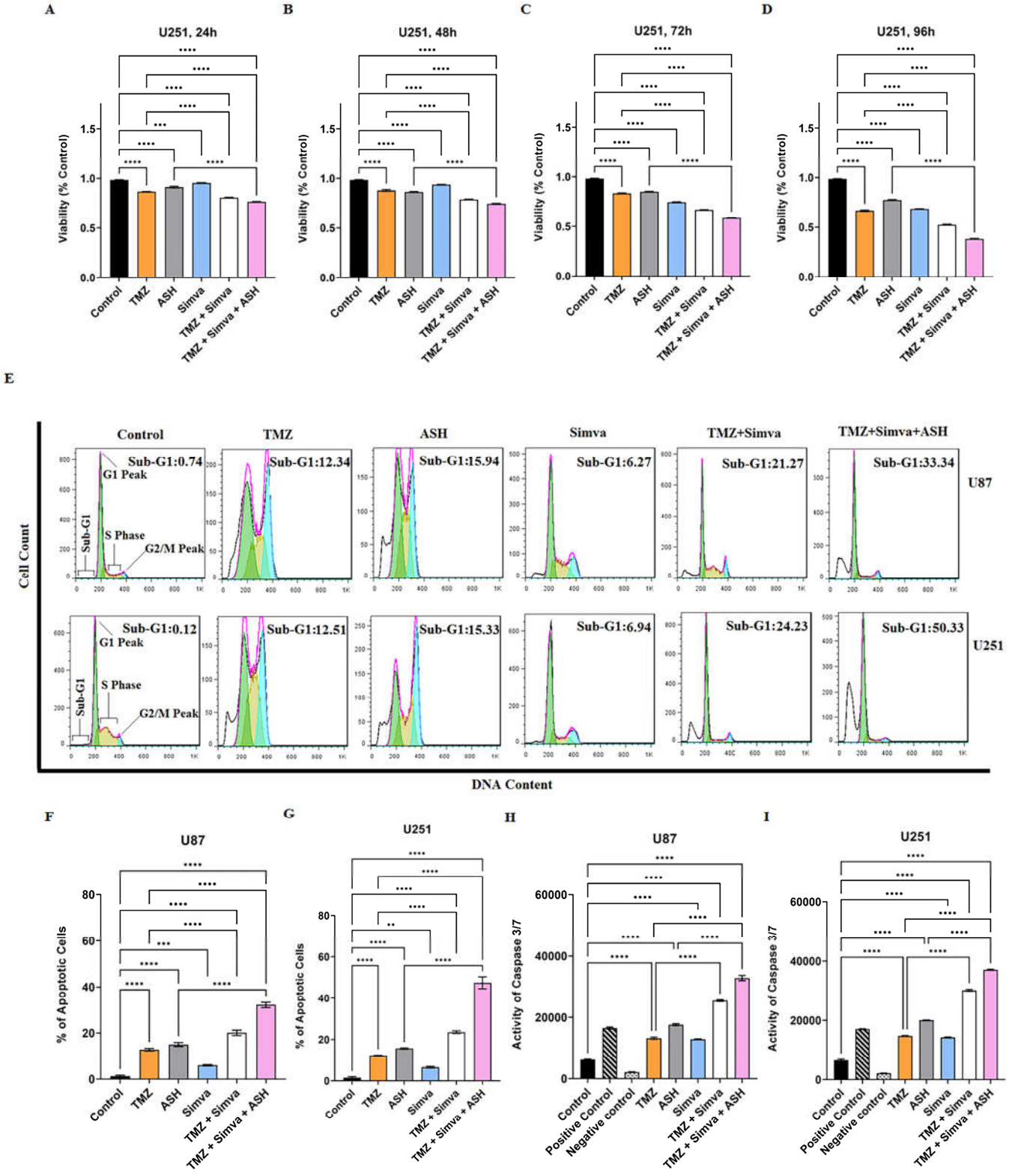

Figure 2. Simvastatin, Temozolomide, Acetylshikonin and their combination treatments induce significant apoptotic cell death in human glioblastoma cells. U251 cells were treated with TMZ 100μM, Simva 1μM, ASH 1.5 μM, TMZ/Simva and TMZ/Simva/ASH at 24, 48, 72 and 96 hrs time points. Cell viability was measured using MTT assay and compared to time match vehicle control. Both combinations induced significant decrease in the cell viability compared to TMZ at all time points (****=P<0.0001). The cytotoxicity of TMZ/Simva/ASH was significantly higher than ASH at all time

Preprints (www.preprints.org) | NOT PEER-REVIEWED | Posted: 13 January 2023 doi:10.20944/preprints202301.0247.v1

points (****=P< 0.0001) (**A-D**). All experiments were done in 9 replicates and three independent biological replicates. The results were shown as mean ±SD. We measured apoptosis using Nicoletti assay at 72h for U87 and U251 cells. The cell cycle pattern of each treatment is shown for both cell lines (**E**). The results showed a significant increase of apoptotic cell population (sub-G1) in TMZ-Simva and TMZ/Simva/ASH treated cells compared to the TMZ treatment alone in both U87 (**F**) and U251 (**G**) cells (****=P<0.0001). Moreover, apoptosis was reinforced in TMZ/Simva/ASH combination to ASH in GBM cells (****=P<0.0001) (**F-G**). Caspase-3/-7 activity was assessed in GBM cells which were treated with TMZ (100 μM), Simva (1μM for U251 and 2.5 μM for U87), and ASH (1.5 μM) at 48h (**H, I**). The activation of caspase-3/-7 was determined by Cayman fluorescence assay kit. All treatments significantly increased caspase-3/-7 activity to untreated U87 (**H**) and U251 (**I**) vehicle time match controls (****=P<0.0001). Caspase-3/-7 activation were significantly higher in both combination treatments (TMZ/Simva, TMZ/Simva/ASH) compared to TMZ and ASH treatments in both U87 (H) and U251 (I) GBM cells (****=P<0.0001).

3.3. TMZ, Simva, ASH, TMZ/Simva and TMZ/Simva/ASH Treatments Increase Reactive Oxygen Species and Decrease Mitochondrial Membrane Potential in GBM Cells.

Presence of ROS and a decrease in mitochondrial membrane potential are hallmarks of apoptosis [24,53,61-64]. Therefore, we have measured the amount of ROS and the mitochondrial membrane potential in different experimental conditions.

We assessed ROS in TMZ, Simva, ASH, TMZ/Simva and TMZ/Simva/ASH treatments at two different time points (38 hrs and 60 hrs). We observed a significant increase of ROS in all treatments in both cell lines and time points in U251 (Figure 3A-D) and U87 (Supplementary Figure 3 A-D) compared to the time match vehicle control (P<0.0001). However, ROS did not significantly increase in the Simva treatment in U87 cells at 60 hrs (Supplementary Figure 3C-D). Both TMZ/Simva and TMZ/Simva/ASH combination treatments significantly increased ROS (P<0.0001) compared to single treatment, except for TMZ/Simva compared to TMZ treatments in U87 at 38 hrs (Supplementary Figure 3B) (P>0.05).

Our investigations also showed that all treatments (TMZ, Simva, ASH, TMZ/Simva and TMZ/Simva/ASH) significantly reduced mitochondrial membrane potential in both U251 (Figure 3E-F) and U87 (Supplementary Figure 3E-F) (P<0.0001). Both combination treatments (TMZ/Simva, TIMZ/Simva/ASH) significantly reduced mitochondrial membrane potential in U251 (Figure 3E-F) and U87 (Supplementary Figure 3E-F) compared to single treatment (P<0.0001).

Preprints (www.preprints.org) | NOT PEER-REVIEWED | Posted: 13 January 2023 doi:10.20944/preprints202301.0247.v1

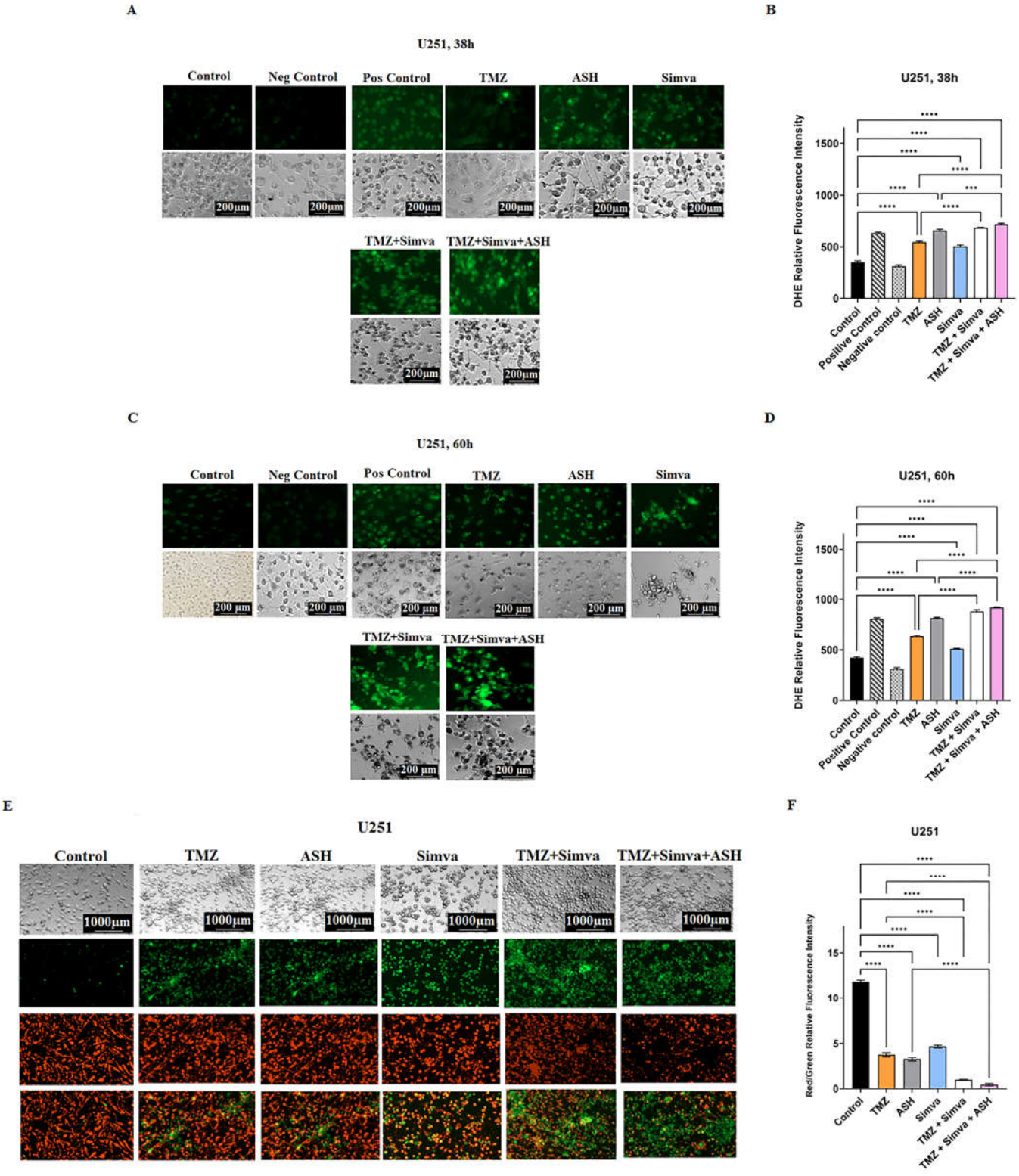

Figure 3. Simvastatin, Temozolomide, Acetylshikonin and their combination treatments induce mitochondrial damage in human glioblastoma cells. U251 cells were treated with TMZ 100µM, Simva 1µM, ASH 1.5 µM, TMZ/Simva and TMZ/Simva/ASH at two different time points (38 and 60 hrs). Cayman ROS detection cell based assay (DHE) was used to assess levels of ROS in different conditions. All treatments induced a significant increase of ROS at both time points compared to the time match control (****=*P*<0.0001). Also, both combinations treatments (TMZ/Simva, TMZ/Simva/ASH) significantly induced more ROS compared to TMZ and ASH single treatments at both time points

 doi:10.20944/preprints202301.0247.v1

(38 and 60 hrs) (***=P<0.001; ****=P<0.0001) (**A-D**). We also measured mitochondria membrane potential (MMP) in the U251 cell line. All treatments (TMZ 100μM, Simva 1μM, ASH 1.5 μM, TMZ-Simva and TMZ-Simva-ASH) induced a significant decrease in MMP compared to the time match control (****=P<0.0001) (**E-F**). Both combination treatments induced a decrease of MMP compared to TMZ and ASH single treatments (****=P<0.0001). All experiments have been done in 3 independent biological replicates.

3.4. The Impact of TMZ, Simva, ASH, TMZ/Simva and TMZ/Simva/ASH Treatments on Autophagy in GBM Cells

Autophagy and apoptosis are interconnected, as autophagy can positively or negatively control apoptosis induction based on the type of stimuli and the cell models [22,65-67]. In our recent investigations we have shown that Simva inhibits the fusion of autophagosomes and lysosomes and increases the apoptotic response to TMZ treatment in GBM cell lines and primary patient-derived GBM tumor cells [33]. Therefore, in our current investigation, we addressed the impact of autophagy in response to TMZ/Simva/ASH combination treatment. We first evaluated AVOs using AO staining in different experimental conditions including TMZ, Simva, ASH, TMZ/Simva and TMZ/Simva/ASH at 72 hrs. The results showed that the number of AVOs significantly increased in all experimental conditions, including TMZ and ASH treatments (statistical significance of P<0.05) and Simva, TMZ/Simva, and TMZ/Simva/ASH treatments (statistical significance of P<0.001) in both U87 and U251 cells (Figure 4A-C). The significant increase of AVO positive cells in combination treatments including Simva and ASH guided us to investigate the potential mechanism that led to this result. In our previous investigation, our team has shown that Simva co-treatment with TMZ increased the number of autophagosomes and AVOs because of the inhibition of autophagosome and lysosome fusion in GBM cells [33]. Our current results showed that a combination of TMZ/Simva/ASH significantly increased the number of AVOs compared to TMZ/Simva treatment (Figure 4A-C).

In the next step, we evaluated the biogenesis of autophagosome and autophagy flux in different experimental conditions (ASH, TMZ/Simva/ASH) using Baf-A1 and inhibition of autophagy flux (5 nM, 72 hrs). The results showed that the ASH treatment did not significantly change LC3β-II/LC3β-I and p62 in both U87 and U251 cells (P>0.05) (Figure 4D, G, H, L, M). In addition, our results showed that there is not any significant difference in LC3β-II/LC3β-I and p62 between Baf-A1 treatment and Baf-A1/ASH (P>0.05) (Figure 4D, G, H, L, M). TMZ/Simva/ASH non-significantly (P>0.05) increased LC3β-II/LC3β-I and p62, while Baf-A1 co-treatment significantly changed LC3β-II/LC3β-I and p62 in both U87 and U251 cells (P<0.01, P<0.001) (Figure 4D, G, H, L, M). Therefore, ASH treatment increases the number of AVO positive cells via fast turnover of autophagosomes while TMZ/Simva/ASH increases AVO positive cells via partial inhibition of autophagy flux in GBM cells (U87 and U251).

Preprints (www.preprints.org) | NOT PEER-REVIEWED | Posted: 13 January 2023 doi:10.20944/preprints202301.0247.v1

A

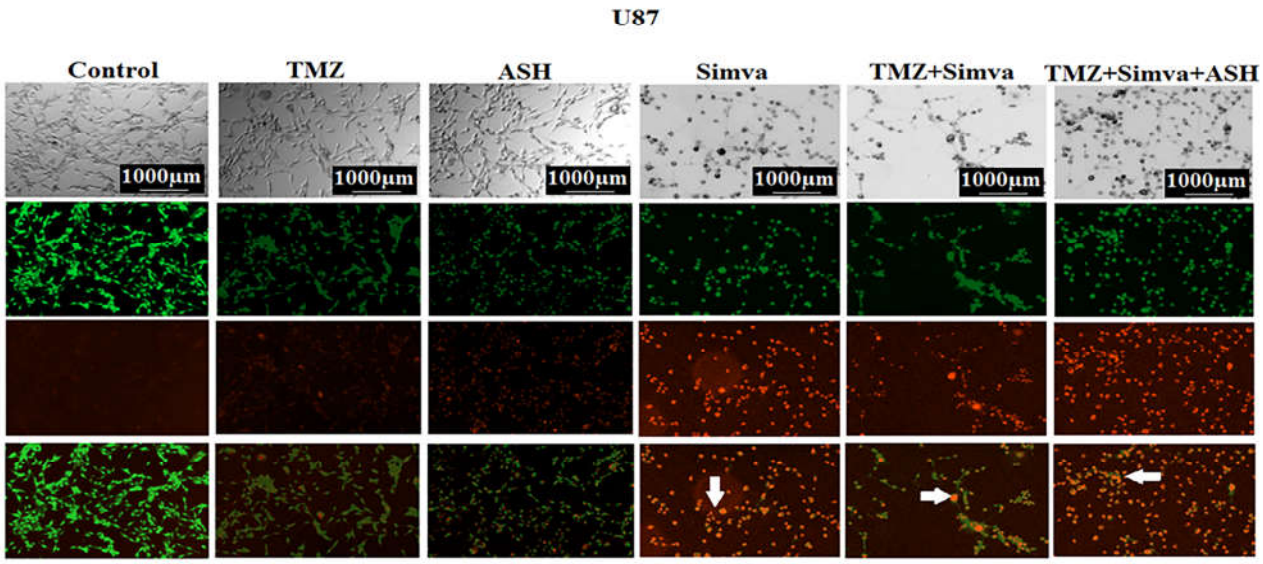

B

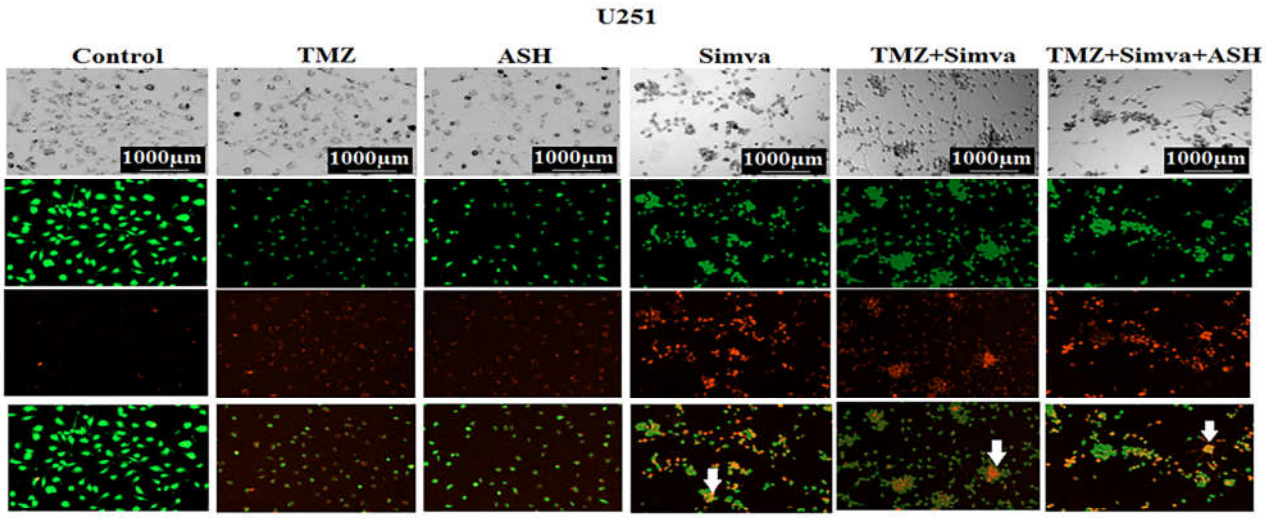

C

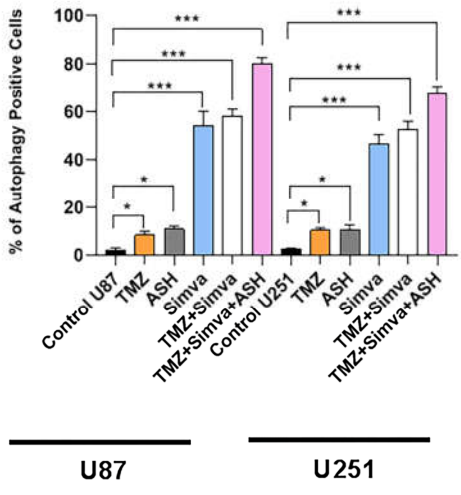

Preprints (www.preprints.org) | NOT PEER-REVIEWED | Posted: 13 January 2023 doi:10.20944/preprints202301.0247.v1

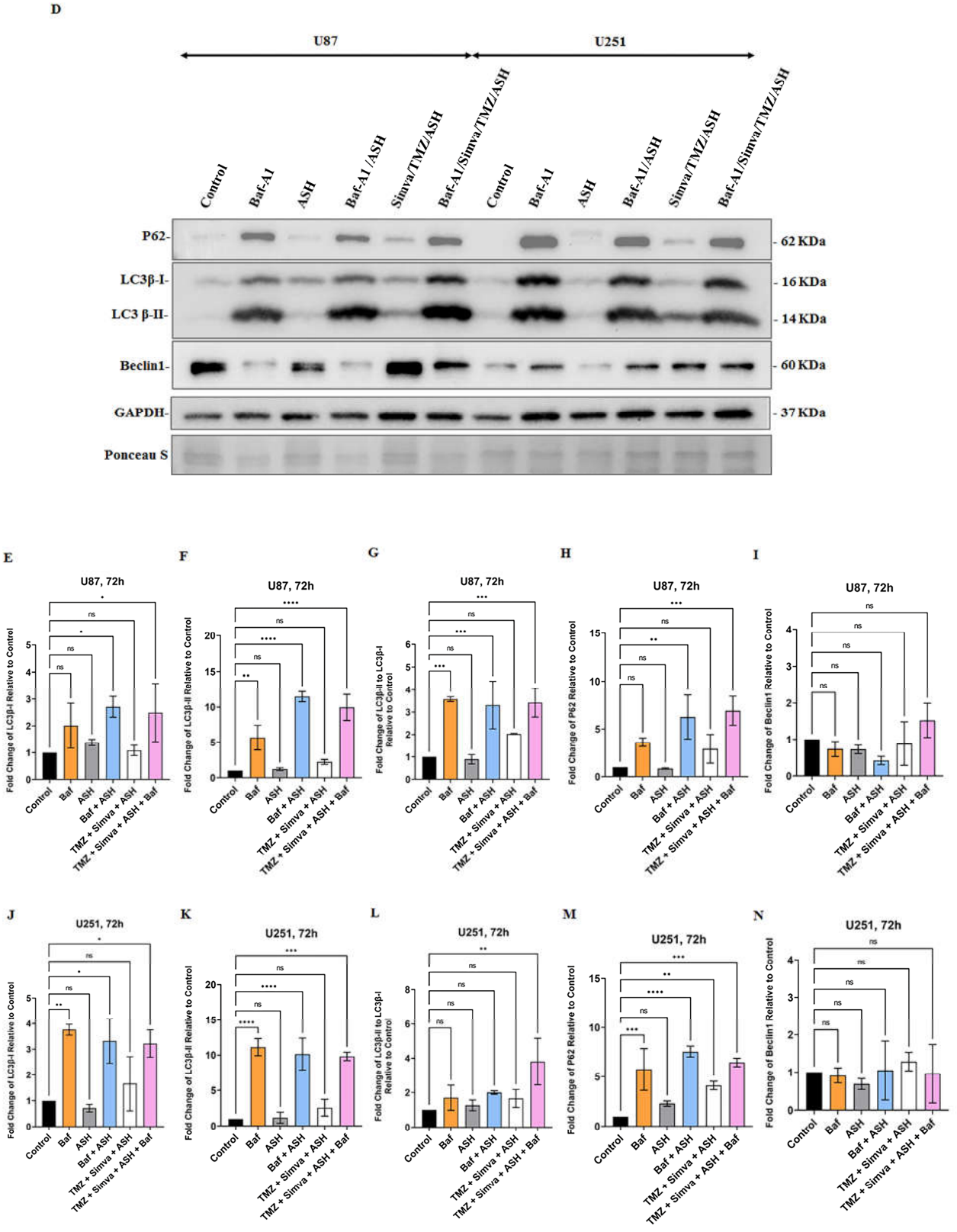

Figure 4. Simvastatin, Temozolomide, and Acetylshikonin combination treatments change autophagy flux in human glioblastoma cells. U87 and U251 cells were treated with TMZ 100μM, Simva (2.5, 1μM respectively), ASH 1.5 μM, TMZ/Simva and TMZ/Simva/ASH for 48 hrs. The formation of acidic vesicular organelles [53] was assessed using acridine orange (AO). The green fluorescence turned to red AVOs in the treatment conditions (white arrows) (**A-B**) [3]. The percentage of AVO

Preprints (www.preprints.org) | NOT PEER-REVIEWED | Posted: 13 January 2023 doi:10.20944/preprints202301.0247.v1

positive cells were evaluated. All treatments significantly increased the percentage of AVO positive cells in both cell lines compared to the time match vehicle control. The cells treated with TMZ/Simva/ASH showed the highest percentage of AVO positive cells (*=P<0.05, ***=P<0.001) (**C**). We further evaluated autophagy in different experimental conditions using immunoblotting. GBM cells were treated with Bafilomycin A1 (autophagy flux inhibitor) (5 nM), ASH, Baf/ASH, TMZ/Simva/ASH and Baf/TMZ/Simva/ASH for 72hrs (all concentrations were the same as AO experiments). p62 degradation, LC3β lipidation and formation of LC3β-II and Beclin-1 expressions were evaluated using immune blotting. Ponceau S was utilized as loading control (**D**). ASH increased the turnover of autophagosomes in both U87 and U251 cells, although it was not statistically significant (**E- H**, **J-M**). Baf significantly increased LC3β-II lipidation and decreased p62 degradation in both U87 and U251 cells, confirming the effect of ASH in autophagy and autophagosome turnover (**E- H**, **J-M**). TMZ/Simva/ASH partially inhibited autophagy flux, which is confirmed by the non-significant increase of LC3β-II and non-significant decrease in p62 degradation. Baf significantly induced LC3β lipidation, and accumulation of p62 in combination with TMZ/Simva/ASH treatment in both U87 and U251 cells (**E-H**, **J-M**) (*ns*: non-significant; *= P< 0.05; **= P<0.01, ***= P<0.001, ****= P< 0.0001).

3.5. Autophagy Flux Inhibition Increases Simva, TMZ, ASH and Combination Triple Treatment-Induced Cell Death in GBM Cells.

We have shown that the TMZ/Simva/ASH combination treatment induced a partial block of the autophagy flux in GBM cells (Figure 4). We further investigated the impact of autophagy flux inhibition in TMZ, Simva, ASH, and TMZ/Simva/ASH-induced cell death in GBM cells. We used chloroquine (CQ) as the autophagy flux inhibitor [68,69]. We first investigated the cytotoxic effects of CQ (25-200 μM) at different time points (24, 48 and 72 hrs) using the MTT assay to optimize the lowest concentration that inhibits the flux and has the lowest cytotoxic effect in GBM cells. The results are summarized in (Figure 5A-C) (U251) and (Supplementary Figure 4A-C) (U87), which show that the least toxic concentration of CQ that still inhibits flux (data was not showed) are 25 μM and 50 μM in U87 and U251 cells, respectively. Therefore, we used a combination of CQ (25 μM for U87, 50 μM for U251) with TMZ (100 μM), Simva (2.5 and 1 μM for U87 and U251, respectively), ASH (1.5 μM) and TMZ/Simva/ASH. CQ (autophagy flux inhibition) in combination with Simva (Figure 5D-F, Supplementary Figure 4D-F), TMZ (Figure 5G-I, Supplementary Figure 4G-I), ASH (Figure 5J-L, Supplementary Figure 4J-L) and TMZ/Simva/ASH (Figure 5M-O, Supplementary Figure 4M-O) significantly (P<0.0001) decreased the cell viability in both U251 and U87 cell lines. Overall, it can be concluded that autophagy flux inhibition increased the triple combination treatment-induced cell death in GBM cells.

Preprints (www.preprints.org) | NOT PEER-REVIEWED | Posted: 13 January 2023 doi:10.20944/preprints202301.0247.v1

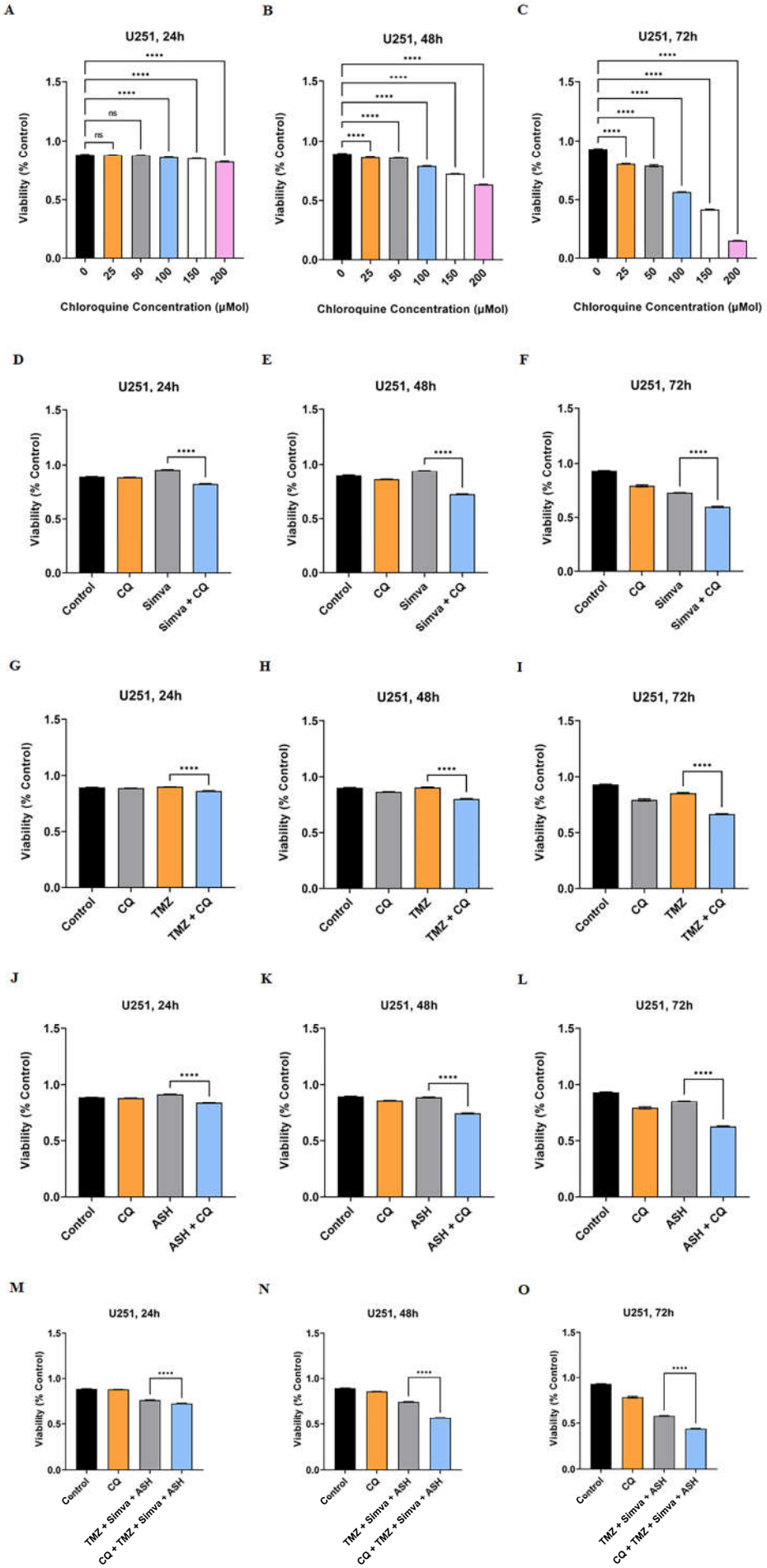

 doi:10.20944/preprints202301.0247.v1

Figure 5. Autophagy flux inhibition increases Simvastatin, Temozolomide, Acetylshikonin and triple combination treatment-induced cell death. U251 cells were treated with different concentrations of chloroquine (CQ) (25-200 μM) at 24, 48 and 72 hrs. Cell viability was assessed via MTT test (**A-C**). CQ induced significant cell death for all concentrations at all time points (****= $P<0.0001$) except 25 and 50 μM concentrations at 24 hrs ($P>0.05$). We used CQ 50 μM in combination with Simva 1 μM (**D-F**), TMZ 100 μM (**G-I**) [98], ASH 1.5 μM (**J-L**) and TMZ/Simva/ASH (**M-O**) for 24, 48, and 72 hrs. CQ decreased cell viability in combination with all treatments (****= $P<0.0001$), which showed that TMZ, Simva, ASH, and TMZ/Simva/ASH-induced cell death is dependent on autophagy flux. All experiments have been done in 9 replicates and three independent biological replicates and are showed as mean ±SD.

3.6. Role of Bcl2 pro- and anti-Apoptotic Family Proteins in TMZ/Simva/ASH Induced Cell Death in GBM cells

Bcl2 family proteins play an important role in the regulation of apoptotic cell death related to mitochondria [63,70,71]. Our results showed that TMZ, Simva, ASH, TMZ/Simva, and TMZ/Simva/ASH treatments increased ROS and decreased mitochondrial membrane potential in U251 (Figure 3A-F) and U87 (Supplementary Figure 3A-F) GBM cells. Our previous investigations showed that Bcl2 family proteins are involved in the regulation of statins and TMZ-induced cell death in GBM cell [31,33]. Our current investigation showed that Baf/TMZ/Simva/ASH combination significantly increased pro-apoptotic protein (Bax) in U87 cells (Figure 6 A, B) ($P< 0.001$) while the treatment non-significantly increased Bax expression in U251 (Figure 6A, F) ($P> 0.05$). On the other hand, TMZ/Simva/ASH did not significantly change the expression of anti-apoptotic proteins (Bcl2, Bcl-XL, Mcl-1) in U87 (Figure 6A, C, D, E) and U251 (Figure 6A, G, H, I) cells ($P>0.05$). Therefore, it can be concluded that TMZ/Simva/ASH-induced cell death in GBM cells is potentially dependent on pro-apoptotic Bax protein expression.

Preprints (www.preprints.org) | NOT PEER-REVIEWED | Posted: 13 January 2023 doi:10.20944/preprints202301.0247.v1

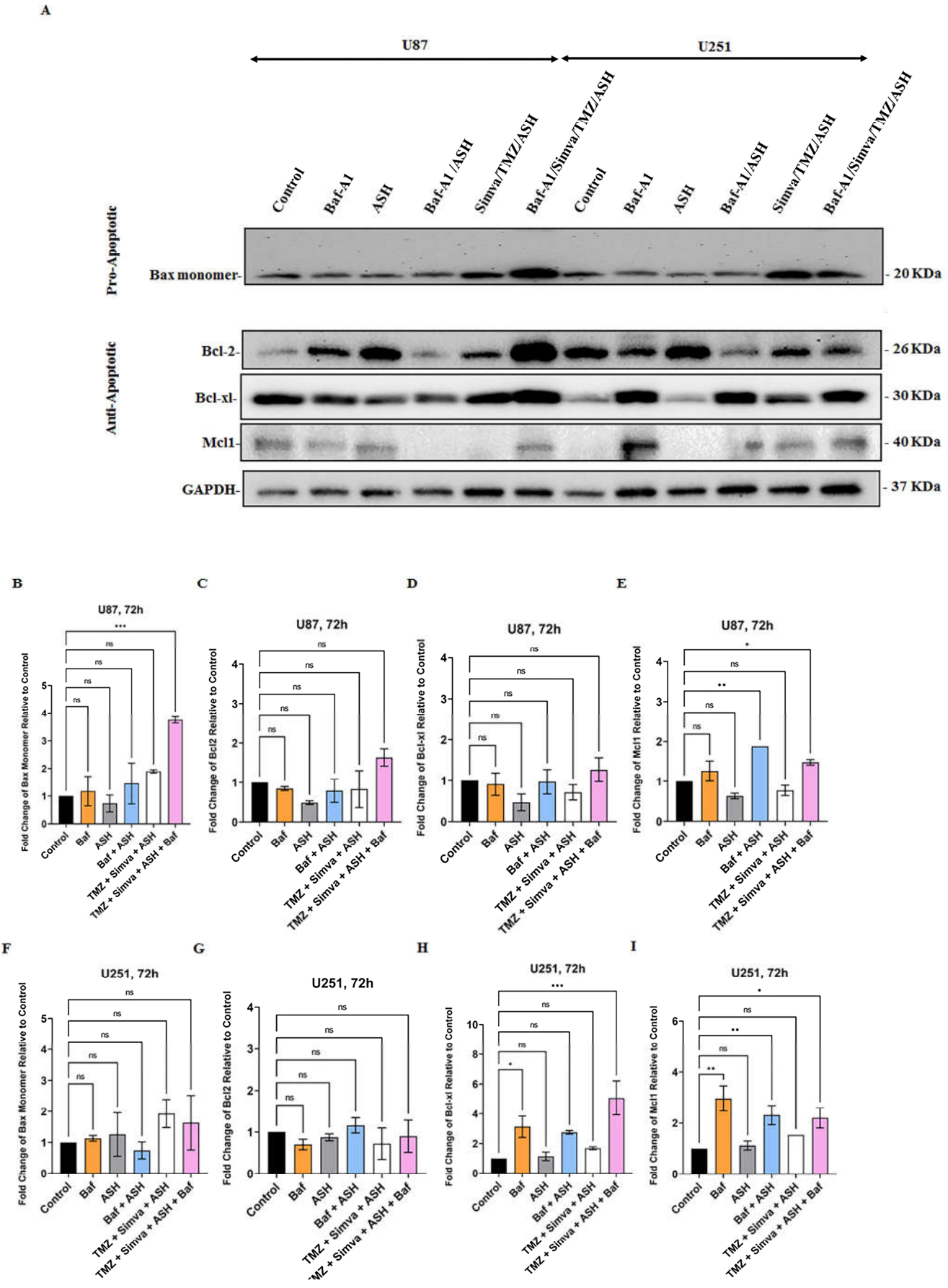

 doi:10.20944/preprints202301.0247.v1

Figure 6. Effect of Autophagy Flux inhibition on pro and anti- apoptotic proteins expressions in GBM cells. We used Bafilomycin A1 (Baf) 5 nM in combination with ASH 1.5 μM and TMZ/Simva/ASH (Simva 1 μM, U251 and Simva 2.5 μM, U87). We evaluated pro- (Bax) and anti-apoptotic Bcl2 (Bcl2, Bcl-XL, Mcl-1) family proteins in different experimental conditions using immunoblotting at 72 hrs. GAPDH was utilized as loading control (**A**). TMZ/Simva/ASH non-significantly increased Bax expression (P>0.05) while TMZ/Simva/ASH/Baf significantly increased Bax expression in U87 cells (***=P<0.001), (**B**). All treatments did not significantly change Bcl2 (**C**) and Bcl-XL (**D**) expressions in U87 cells. The Baf treatment significantly increased Mcl-1 expression in both ASH (P<0.01) and TMZ/Simva/ASH (*=P<0.05) treatments in U87 cells (**E**). TMZ/Simva/ASH and its combination with Baf non-significantly increased Bax expression (P>0.05) in U251 cells (**F**). All treatments did not significantly change Bcl2 (**G**) expression in U251 cells. Baf treatment significantly increased Bcl-XL (**H**) expression in U251 cells (single Baf treatment, P<0.05, Baf-TMZ/Simva/ASH, P<0.001). Baf treatment significantly increased Mcl-1 (**I**) expression in U251 cells (single Baf treatment, P<0.01, Baf-TMZ/Simva/ASH, P<0.05). All experiments have been done in 9 replicates and three independent biological replicates and are shown as mean ±SD.

4. Discussion

Many chemotherapy approaches are not effective towards reaching the desired outcomes in GBM patient treatment [72,73] . Our team has recently investigated the efficiency and mechanisms of combination Simva and TMZ treatments in GBM and showed that Simva sensitizes GBM cells to TMZ-induced apoptosis [10,20,22]. TMZ resistance, as a major problem in GBM patient therapeutic strategies, has been investigated for years. Moreover, several compounds and drugs were utilized to enhance the efficacy of TMZ while attenuate the resistance to TMZ to achieve the best approach to treat GBM patients [72-74]. Recent investigations have showed that taking statins for a long period of time, could potentially increase the survival of the cancer patients (including GBM) and improve their response to different chemotherapy medications [9,75-77]. A significant synergistic effect of statins has been reported in combination with chemotherapy compounds including cisplatin, 5-Fluorouracil (5-FU), doxorubicin and paclitaxel [78]. A recent investigation has also showed that lovastatin sensitizes GBM cells (U251 and U87) to TMZ-induced apoptosis via inhibition of autophagy flux [79]. These results support our recent findings about the mechanisms of sensitization of GBM cells to TMZ-induced apoptosis using Simva [33]. Several other investigations have showed that simvastatin induces apoptosis in breast cancer, chronic myeloid leukemia (CML) and lung cancer cells via changing the balance between pro- and anti-apoptotic Bcl2 family proteins [78]. Co-treatment of Simva and flavons decreases chemo-resistance to doxorubicine via degradation of multi drug resistance (MDR) proteins in human colon cancer cells [80]. In another investigation, it has been showed that liposomal Simva sensitizes C26 colon carcinoma cells to liposomal 5-FU via inhibition of tumor angiogenesis in vivo [81]. Simvastatin also sensitizes A549 non-small cell lung cancer to Sulindac, or Pemetrexed (multi-target antifolate medication) induced caspase-dependent apoptosis via damaging mitochondria and increasing ROS [82,83].

Our previous studies revealed that simvastatin triggers the intrinsic apoptosis in various human cancer cells including GBM via inhibition of the mevalonate cascade with subsequent targeting of geranylgerany pyrophosphate prenylation precursors [84]. We later showed that the TMZ/Simva combination treatment increased apoptosis compared to the TMZ and Simva single treatments in GBM cells. Our investigations showed that Simva sensitizes GBM cells and GBM patient-derived tumor cells to TMZ-induced apoptosis via inhibition of autophagy flux and UPR induction [33,55].

In the current investigation, for the first time, we have assessed mechanisms of ASH-induced apoptosis and later provided mechanisms which are involved in TMZ/Simva/ASH-induced apoptosis in GBM cells. In summary, our results showed that ASH and its triple combination treatment (TMZ/Simva/ASH) increased cellular ROS, decreased mitochondrial membrane potential with subsequent caspase-dependent apoptosis induction in GBM cells. In addition, our results showed that ASH induced autophagy while TMZ/Simva/ASH partially inhibited autophagy flux in GBM cells. Furthermore,

 doi:10.20944/preprints202301.0247.v1

blocking autophagy flux increased ASH and TMZ/Simva/ASH-induced cell death in GBM cells which clearly shows that both ASH and TMZ/Simva/ASH-induced cell death are dependent on the autophagy pathway.

ASH induces apoptosis in a wide range of tumor cells, such as ROS-dependent apoptosis in oral squamous cell carcinoma cells (Ca9-22) [7]. Recent investigations have shown that ASH increases ROS and nuclear damage with subsequent nuclear translocation of FOXO3 and induced caspase-dependent apoptosis in osteosarcoma U2OS, renal cell carcinoma and colorectal cancer HCT-15, and LoVo cells [85-87]. It has also been reported that ASH induces dose-dependent apoptosis via activation of caspase-3/-7 and -9 in chondrosarcoma cell lines [88]. They also showed that MAPK activation is involved in ASH-induced apoptosis in colorectal cancer cells [88]. On the other hand, ASH induces caspase-dependent apoptosis via ROS and inhibition of NF-κB in K562 leukemia cells [89]. The combination of Erlotinib and Shikonin (and its derivatives) has been recently assessed in GBM cells. The cytotoxicity results showed a synergic effect of Shikonin and its derivatives including ASH with Erlotinib in GBM cells (U87, BS153, A431 and DK-MG) [90]. In conclusion, the ASH-induced ROS hampers tumor cell proliferation, leading to the caspase-dependent apoptosis in cancer cells including GBM cells. In addition, combination therapy with Shikonin or its derivatives improves the response of cancer cells to chemotherapy agents and induces higher apoptotic cell death compared to single chemotherapy strategies.

Previous investigations have shown that an increase of pro-apoptotic Bcl2 family proteins or decrease in anti-apoptotic Bcl2 protein expression might be involved in mitochondrial damage, increase in cellular ROS and decrease in mitochondrial membrane potential [31,46,49,70,91-93]. It has been showed that ASH induces apoptosis in osteosarcoma U2OS cells , A498 and ACHN (human RCC cell lines), colorectal Cancer HCT-15 and LoVo cells, and human leukemia cell line K562, via changing the Bcl2 family proteins [85-87,89]. Interestingly, our investigations showed that ASH did not significantly change Bax, Bcl2, Bcl-XL and Mcl-1 expression while it decreased mitochondrial membrane potential, increased ROS, activated caspase-3/-7 and induced apoptosis in GBM cell lines (U87 and U251). In addition, our investigation has revealed for the first time that TMZ/Simva/ASH induces mitochondria-dependent apoptosis without significant changes in the expression of anti-apoptotic Bcl2 family proteins (Bcl2, Bcl-XL, and Mcl-1), while non-significantly increasing Bax pro-apoptotic protein in U87 and U251 cells. Therefore, our findings indicate that ASH and TMZ/Simva/ASH mitochondria-induced apoptosis in GBM cells might be dependent on other Bcl2 family proteins or could be triggered by other mitochondrial factors like Smac/Diablo, Omi/HtrA2 [70]. Interestingly, Bafilomycin-A1 increases anti-apoptotic protein Mcl-1 in both U87 and U251 cells and Bcl-XL expression in U251 cells (which could not be mechanistically explained and needs further investigations to justify its mechanisms).

In our recent investigations, our team has showed that autophagy is a regulator for apoptosis induction in different types of cells including airway mesenchymal cells [49,53,71], atrial fibroblasts [94], primary cardiac myofibroblasts [53], human alveolar rhabdomyosarcoma cells [8], HCT116, colorectal cancer cell line [47,48] and GBM cells [33]. Recent investigations have also showed that ASH induces autophagy via PI3/AKT pathway which controls its apoptosis induction in acute myeloid leukaemia (AML) cells [95]. Our current investigations also showed that ASH induces simultaneous autophagy and apoptosis, and autophagy flux inhibition increases ASH-induced cell death in GBM cells. For the first time, we have also showed that TMZ/Simva/ASH partially inhibits autophagy flux in GBM cells while further induction of autophagy flux inhibition significantly increased triple combination therapy-induced cell death in these cells. Overall, our investigations showed that autophagy flux plays an important role in both ASH and TMZ/Simva/ASH-induced cell death in GBM cell lines.

In our future investigations, we will try to address the impact of UPR in TMZ/Simva/ASH-induced apoptosis as it has been recently showed that UPR is involved in ASH-induced apoptosis [96]. In addition, we will use the backbone of our recent Simva-

loaded nanoparticle which specifically binds to GBM cells [97]. We will attempt to load both Simva and ASH on these nanoparticles to increase the efficiency of targeting GBM with triple combination therapy. We will also move towards both flank and xenograft GBM animal model to test different combination therapies and investigate the impact of these approaches on animal models and be closer to clinical applications of these medications.

5. Conclusions

In this study, we assessed the efficacy of TMZ-Simva-ASH combination on GBM cancer cells compared to single therapies. The changes in the cell viability, sub-G1 cell population, ROS levels, caspases activation and mitochondria membrane potential were explored to demonstrate the apoptosis cell death. AVOs, LC3II and p62 markers were also examined as the main autophagy markers. According to the findings, TMZ and ASH and t induced both mitochondrial apoptosis and autophagy. The triple combination treatment induced apoptosis and partially inhibits autophagy flux. Moreover, the triple treatment-induced apoptosis was significantly higher than the single therapies. Our results also showed that TMZ, Simva, ASH, TMZ/Simva/ASH-induced apoptosis increases via autophagy flux inhibition

Supplementary Materials: Figure S1: Simvastatin, Temozolomide and Acetylshikonin treatments induce cell death in human glioblastoma cells; Figure S2: Simvastatin, Temozolomide, Acetylshikonin and their combination treatment induce significant cell death in human glioblastoma cells; Figure S3: Simvastatin, Temozolomide Acetylshikonin and their combination treatment induce mitochondrial damage in human glioblastoma cells; Figure S4: Autophagy flux inhibition increases Simvastatin, Temozolomide, Acetylshikonin and triple combination treatment-induced cell death.

Author Contributions: All authors read and approved the final manuscript. Sima Hajiahmadi did the MTT assay, flow cytometry, AO, caspase-3/-7 assay, ROS and MMP assays and drafted the manuscript. Rosa Iranpour and Shahrokh Lorzadeh did immune blotting, autophagy flux inhibition assay, and immune blotting quantification and graph preparation. Saeed Karima and Masoumeh Rajabibazl contributed in methodology (FACS, AO assay). Zahra Shahsavari and Saeid Ghavami, designed the whole project, provided funding and made final proof read of article and supervise the whole project.

Funding: Please add: SG was support via UCRP operating grant number 54304. Rosa Iranpour stipend was supported by University of Manitoba undergraduate award.

Institutional Review Board Statement: Not applicable.

Informed Consent Statement: Not applicable.

Data Availability Statement: All original data for immune blotting has been upload to MDPI website. The other data presented in this study are available upon request from the corresponding authors.

Acknowledgments: This article has been extracted from the Ph.D. thesis written by Mrs. Sima Hajiahmadi in the Faculty of Medicine, Shahid Beheshti University of Medical Sciences. The authors acknowledge Dr. Pooneh Mokarram (SUMS) and Dr. Ahmad Nasimian for their technical support.

Conflicts of Interest: The authors declare no conflict of interest.

References

1. Pirmoradi, L.; Seyfizadeh, N.; Ghavami, S.; Zeki, A.A.; Shojaei, S. Targeting cholesterol metabolism in glioblastoma: a new therapeutic approach in cancer therapy. *J Investig Med.* **2019**, *67*, 715-719, doi: 10.1136/jim-2018-000962.
2. Johannessen, T.C.; Hasan-Olive, M.M.; Zhu, H.; Denisova, O.; Grudic, A.; Latif, M.A.; Saed, H.; Varughese, J.K.; Røsland, G.V.; Yang, N. Thioridazine inhibits autophagy and sensitizes glioblastoma cells to temozolomide. *Int J cancer.* **2019**, *144*, 1735-1745, doi: 10.1002/ijc.31912.
3. Grochans, S.; Cybulska, A.M.; Simińska, D.; Korbecki, J.; Kojder, K.; Chlubek, D.; Baranowska-Bosiacka, I. Epidemiology of Glioblastoma Multiforme–Literature Review. *Cancers.* **2022**, *14*, 2412, doi: 10.3390/cancers14102412.

4. Liao, W.; Fan, S.; Zheng, Y.; Liao, S.; Xiong, Y.; Li, Y.; Liu, J. Recent advances on glioblastoma multiforme and nano-drug carriers: A review. *Curr Med Chem.* **2019**, *26*, 5862-5874, doi: 10.2174/0929867325666180514113136.
5. Cruz, J.V.R.; Batista, C.; Afonso, B.H.; Alexandre-Moreira, M.S.; Dubois, L.G.; Pontes, B.; Moura Neto, V.; Mendes, F.A. Obstacles to Glioblastoma Treatment Two Decades after Temozolomide. *Cancers (Basel)* **2022**, *14*, 3203, doi: 10.3390/cancers14133203.
6. McMahon, D.J.; Gleeson, J.P.; O'Reilly, S.; Bambury, R.M. Management of newly diagnosed glioblastoma multiforme: current state of the art and emerging therapeutic approaches. *Med Oncol.* **2022**, *39*, 129, doi: 10.1007/s12032-022-01708-w.
7. Lee, J.H.; Park, H.R.; Choi, Y.W. Acetylshikonin inhibits growth of oral squamous cell carcinoma by inducing apoptosis. *Arch Oral Biol.* **2016**, *70*, 149-157, doi:10.1016/j.archoralbio.2016.06.020.
8. Moghadam, A.R.; da Silva Rosa, S.C.; Samiei, E.; Alizadeh, J.; Field, J.; Kawalec, P.; Thliveris, J.; Akbari, M.; Ghavami, S.; Gordon, J.W. Autophagy modulates temozolomide-induced cell death in alveolar Rhabdomyosarcoma cells. *Cell Death Discov.* **2018**, *4*, 1-16, doi: 10.1038/s41420-018-0115-9.
9. Shojaei, S.; Alizadeh, J.; Thliveris, J.; Koleini, N.; Kardami, E.; Hatch, G.M.; Xu, F.; Hombach-Klonisch, S.; Klonisch, T.; Ghavami, S. Statins: a new approach to combat temozolomide chemoresistance in glioblastoma. *J Investig Med.* **2018**, *66*, 1083-1087, doi: 10.1136/jim-2018-000874.
10. Shojaei, S.; Koleini, N.; Samiei, E.; Aghaei, M.; Cole, L.K.; Alizadeh, J.; Islam, M.I.; Vosoughi, A.r.; Albokashy, M.; Butterfield, Y. Simvastatin increases temozolomide-induced cell death by targeting the fusion of autophagosomes and lysosomes. *FEBS J.* **2020**, *287*, 1005-1034, doi: 10.1111/febs.15069.
11. Lin, C.-J.; Lee, C.-C.; Shih, Y.-L.; Lin, T.-Y.; Wang, S.-H.; Lin, Y.-F.; Shih, C.-M. Resveratrol enhances the therapeutic effect of temozolomide against malignant glioma in vitro and in vivo by inhibiting autophagy. *Free Radic Biol Med.* **2012**, *52*, 377-391, doi: 10.1016/j.freeradbiomed.2011.10.487.
12. Ghavami, S.; Zamani, M.; Ahmadi, M.; Erfani, M.; Dastghaib, S.; Darbandi, M.; Darbandi, S.; Vakili, O.; Siri, M.; Grabarek, B.O.; et al. Epigenetic regulation of autophagy in gastrointestinal cancers. *Biochim Biophys Acta Mol Basis Dis* **2022**, *1868*, 166512, doi:10.1016/j.bbadis.2022.166512.
13. Sharma, P.; Alizadeh, J.; Juarez, M.; Samali, A.; Halayko, A.J.; Kenyon, N.J.; Ghavami, S.; Zeki, A.A. Autophagy, Apoptosis, the Unfolded Protein Response, and Lung Function in Idiopathic Pulmonary Fibrosis. *Cells.* **2021**, *10*, 1642, doi: 10.3390/cells10071642.
14. Chen, Y.M.; Burrough, E. The Effects of Swine Coronaviruses on ER Stress, Autophagy, Apoptosis, and Alterations in Cell Morphology. *Pathogens* **2022**, *11*, 940, doi: 10.3390/pathogens11080940.
15. Saptarshi, N.; Porter, L.F.; Paraoan, L. PERK/EIF2AK3 integrates endoplasmic reticulum stress-induced apoptosis, oxidative stress and autophagy responses in immortalised retinal pigment epithelial cells. *Sci Rep* **2022**, *12*, 13324, doi: 10.1038/s41598-022-16909-6.
16. Hsieh, M.J.; Chien, S.Y.; Lin, J.T.; Yang, S.F.; Chen, M.K. Polyphyllin G induces apoptosis and autophagy cell death in human oral cancer cells Phytomedicine. *Phytomedicine.* **2016**, *23*, 1545-1554, doi:10.1016/j.phymed.2016.12.011.
17. Kataura, T.; Sedlackova, L.; Otten, E.G.; Kumari, R.; Shapira, D.; Scialo, F.; Stefanatos, R.; Ishikawa, K.I.; Kelly, G.; Seranova, E.; et al. Autophagy promotes cell survival by maintaining NAD levels. *Dev Cell* **2022**, *57*, 2584-2598 e2511, doi:10.1016/j.devcel.2022.10.008.
18. Fairlie, W.D.; Tran, S.; Lee, E.F. Crosstalk between apoptosis and autophagy signaling pathways. *Int Rev Cell Mol Biol* **2020**, *352*, 115-158, doi: 10.1016/bs.ircmb.2020.01.003.
19. Kawalec, P.; Martens, M.D.; Field, J.T.; Mughal, W.; Caymo, A.M.; Chapman, D.; Xiang, B.; Ghavami, S.; Dolinsky, V.W.; Gordon, J.W. Differential impact of doxorubicin dose on cell death and autophagy pathways during acute cardiotoxicity. *Toxicol Appl Pharmacol* **2022**, *453*, 116210, doi:10.1016/j.taap.2022.116210.
20. Dastghaib, S.; Shojaei, S.; Mostafavi-Pour, Z.; Sharma, P.; Patterson, J.B.; Samali, A.; Mokarram, P.; Ghavami, S. Simvastatin Induces Unfolded Protein Response and Enhances Temozolomide-Induced Cell Death in Glioblastoma Cells, *Cells* **2020**, *9*, 2339. doi: 10.3390/cells9112339.
21. Nikoletopoulou, V.; Markaki, M.; Palikaras, K.; Tavernarakis, N. Crosstalk between apoptosis, necrosis and autophagy. *Biochim Biophys Acta* **2013**, *1833*, 3448-3459, doi: 10.1016/j.bbamcr.2013.06.001.
22. Samiei, E.; Seyfoori, A.; Toyota, B.; Ghavami, S.; Akbari, M. Investigating Programmed Cell Death and Tumor Invasion in a Three-Dimensional (3D) Microfluidic Model of Glioblastoma. *Int J Mol Sci* **2020**, *21*, 3162, doi: 10.3390/ijms21093162.
23. Emami, A.; Shojaei, S.; da Silva Rosa, S.C.; Aghaei, M.; Samiei, E.; Vosoughi, A.R.; Kalantari, F.; Kawalec, P.; Thliveris, J.; Sharma, P.; et al. Mechanisms of simvastatin myotoxicity: The role of autophagy flux inhibition. *Eur J Pharmacol* **2019**, *862*, 172616, doi:10.1016/j.ejphar.2019.172616.
24. Nagakannan, P.; Iqbal, M.A.; Yeung, A.; Thliveris, J.A.; Rastegar, M.; Ghavami, S.; Eftekharpour, E. Perturbation of redox balance after thioredoxin reductase deficiency interrupts autophagy-lysosomal degradation pathway and enhances cell death in nutritionally stressed SH-SY5Y cells. *Free Radic Biol Med* **2016**, *101*, 53-70, doi:10.1016/j.freeradbiomed.2016.09.026.
25. Ahmadi, M.; Amiri, S.; Pecic, S.; Machaj, F.; Rosik, J.; Los, M.J.; Alizadeh, J.; Mahdian, R.; da Silva Rosa, S.C.; Schaafsma, D.; et al. Pleiotropic effects of statins: A focus on cancer. *Biochim Biophys Acta Mol Basis Dis* **2020**, *1866*, 165968, doi:10.1016/j.bbadis.2020.165968.
26. Wen Jiang, Jin-Wei Hu, Xu-Ran He, Wei-Lin Jin, Xin-Yang He. Statins: a repurposed drug to fight cancer. *J Exp Clin Cancer Res* **2021**, *40*, 241, doi: 10.1186/s13046-021-02041-2.

27. Nielsen, S.F.; Nordestgaard, B.G.; Bojesen, S.E. Statin use and reduced cancer-related mortality. *N Engl J Med* **2012**, *367*, 1792-1802, doi: 10.1056/NEJMoa1201735.
28. Gobel, A.; Riffel, R.M.; Hofbauer, L.C.; Rachner, T.D. The mevalonate pathway in breast cancer biology. *Cancer Lett* **2022**, *542*, 215761, doi:10.1016/j.canlet.2022.215761.
29. Marciano, G.; Palleria, C.; Casarella, A.; Rania, V.; Basile, E.; Catarisano, L.; Vocca, C.; Bianco, L.; Pelaia, C.; Cione, E.; et al. Effect of Statins on Lung Cancer Molecular Pathways: A Possible Therapeutic Role. *Pharmaceuticals (Basel)* **2022**, *15*, 589, doi: 10.3390/ph15050589.
30. Gaist, D.; Hallas, J.; Friis, S.; Hansen, S.; Sorensen, H.T. Statin use and survival following glioblastoma multiforme. *Cancer Epidemiol* **2014**, *38*, 722-727, doi:10.1016/j.canep.2014.09.010.
31. Alizadeh, J.; Zeki, A.A.; Mirzaei, N.; Tewary, S.; Rezaei Moghadam, A.; Glogowska, A.; Nagakannan, P.; Eftekharpour, E.; Wiechec, E.; Gordon, J.W.; et al. Mevalonate Cascade Inhibition by Simvastatin Induces the Intrinsic Apoptosis Pathway via Depletion of Isoprenoids in Tumor Cells. *Sci Rep* **2017**, *7*, 44841, doi: 10.1038/srep44841.
32. Sheikholeslami, K.; Ali Sher, A.; Lockman, S.; Kroft, D.; Ganjibakhsh, M.; Nejati-Koshki, K.; Shojaei, S.; Ghavami, S.; Rastegar, M. Simvastatin Induces Apoptosis in Medulloblastoma Brain Tumor Cells via Mevalonate Cascade Prenylation Substrates. *Cancers (Basel)* **2019**, *11*, 994, doi: 10.3390/cancers11070994.
33. Shojaei, S.; Koleini, N.; Samiei, E.; Aghaei, M.; Cole, L.K.; Alizadeh, J.; Islam, M.I.; Vosoughi, A.R.; Albokashy, M.; Butterfield, Y.; et al. Simvastatin increases temozolomide-induced cell death by targeting the fusion of autophagosomes and lysosomes. *FEBS J* **2020**, *287*, 1005-1034, doi:10.1111/febs.15069.
34. Zorman, J.; Sušjan, P.; Hafner-Bratkovič, I. Shikonin suppresses NLRP3 and AIM2 inflammasomes by direct inhibition of caspase-1. *PloS one* **2016**, *11*, e0159826, doi: 10.1371/journal.pone.0159826.
35. Matias, D.; Balça-Silva, J.; Dubois, L.G.; Pontes, B.; Ferrer, V.P.; Rosário, L.; do Carmo, A.; Echevarria-Lima, J.; Sarmento-Ribeiro, A.B.; Lopes, M.C. Dual treatment with shikonin and temozolomide reduces glioblastoma tumor growth, migration and glial-to-mesenchymal transition. *Cell Oncol* **2017**, *40*, 247-261, doi: 10.1007/s13402-017-0320-1.
36. Chen, Q.; Han, H.; Lin, F.; Yang, L.; Feng, L.; Lai, X.; Wen, Z.; Yang, M.; Wang, C.; Ma, Y.; et al. Novel shikonin derivatives suppress cell proliferation, migration and induce apoptosis in human triple-negative breast cancer cells via regulating PDK1/PDHC axis. *Life Sci* **2022**, *310*, 121077, doi:10.1016/j.lfs.2022.121077.
37. Peng, J.; Hu, X.; Fan, S.; Zhou, J.; Ren, S.; Sun, R.; Chen, Y.; Shen, X.; Chen, Y. Inhibition of Mitochondrial Biosynthesis Using a "Right-Side-Out" Membrane-Camouflaged Micelle to Facilitate the Therapeutic Effects of Shikonin on Triple-Negative Breast Cancer. *Adv Healthc Mater* **2022**, *11*, e2200742, doi:10.1002/adhm.202200742.
38. Martelli, A.; Omrani, M.; Zarghooni, M.; Citi, V.; Brogi, S.; Calderone, V.; Sureda, A.; Lorzadeh, S.; da Silva Rosa, S.C.; Grabarek, B.O.; et al. New Visions on Natural Products and Cancer Therapy: Autophagy and Related Regulatory Pathways. *Cancers (Basel)* **2022**, *14*, 5839, doi: 10.3390/cancers14235839.
39. Wu, H.; Xie, J.; Pan, Q.; Wang, B.; Hu, D.; Hu, X. Anticancer agent shikonin is an incompetent inducer of cancer drug resistance. *PloS one* **2013**, *8*, e52706, doi: 10.1371/journal.pone.0052706.
40. Wang, Y.; Hao, F.; Nan, Y.; Qu, L.; Na, W.; Jia, C.; Chen, X. PKM2 Inhibitor Shikonin Overcomes the Cisplatin Resistance in Bladder Cancer by Inducing Necroptosis. *Int J Biol Sci* **2018**, *14*, 1883-1891, doi:10.7150/ijbs.27854.
41. Xiong, W.; Luo, G.; Zhou, L.; Zeng, Y.; Yang, W. In vitro and in vivo antitumor effects of acetylshikonin isolated from Arnebia euchroma (Royle) Johnst (Ruanzicao) cell suspension cultures. *Chin Med* **2009**, *4*, 1-7, doi: 10.1186/1749-8546-4-14.
42. Werner, M.; Lyu, C.; Stadlbauer, B.; Schrader, I.; Buchner, A.; Stepp, H.; Sroka, R.; Pohla, H. The role of Shikonin in improving 5-aminolevulinic acid-based photodynamic therapy and chemotherapy on glioblastoma stem cells. *Photodiagnosis Photodyn Ther* **2022**, *39*, 102987, doi:10.1016/j.pdpdt.2022.102987.
43. Matias, D.; Balca-Silva, J.; Dubois, L.G.; Pontes, B.; Ferrer, V.P.; Rosario, L.; do Carmo, A.; Echevarria-Lima, J.; Sarmento-Ribeiro, A.B.; Lopes, M.C.; et al. Dual treatment with shikonin and temozolomide reduces glioblastoma tumor growth, migration and glial-to-mesenchymal transition. *Cell Oncol (Dordr)* **2017**, *40*, 247-261, doi: 10.1007/s13402-017-0320-1.
44. Alizadeh, J.; Glogowska, A.; Thliveris, J.; Kalantari, F.; Shojaei, S.; Hombach-Klonisch, S.; Klonisch, T.; Ghavami, S. Autophagy modulates transforming growth factor beta 1 induced epithelial to mesenchymal transition in non-small cell lung cancer cells. *Biochim Biophys Acta Mol Cell Res* **2018**, *1865*, 749-768, doi: 10.1016/j.bbamcr.2018.02.007.
45. Hashemi, M.; Ghavami, S.; Eshraghi, M.; Booy, E.P.; Los, M. Cytotoxic effects of intra and extracellular zinc chelation on human breast cancer cells. *Eur J Pharmacol* **2007**, *557*, 9-19, doi: 10.1016/j.ejphar.2006.11.010.
46. Ghavami, S.; Asoodeh, A.; Klonisch, T.; Halayko, A.J.; Kadkhoda, K.; Kroczak, T.J.; Gibson, S.B.; Booy, E.P.; Naderi-Manesh, H.; Los, M. Brevinin-2R1 semi-selectively kills cancer cells by a distinct mechanism, which involves the lysosomal-mitochondrial death pathway. *J Cell Mol Med* **2008**, *12*, 1005-1022, doi: 10.1111/j.1582-4934.2008.00129.x.
47. Siri, M.; Behrouj, H.; Dastghaib, S.; Zamani, M.; Likus, W.; Rezaie, S.; Hudecki, J.; Khazayel, S.; Los, M.J.; Mokarram, P.; et al. Casein Kinase-1-Alpha Inhibitor (D4476) Sensitizes Microsatellite Instable Colorectal Cancer Cells to 5-Fluorouracil via Authophagy Flux Inhibition. *Arch Immunol Ther Exp (Warsz)* **2021**, *69*, 26, doi: 10.1007/s00005-021-00629-2.
48. Behrouj, H.; Seghatoleslam, A.; Mokarram, P.; Ghavami, S. Effect of casein kinase 1alpha inhibition on autophagy flux and the AKT/phospho-beta-catenin (S552) axis in HCT116, a RAS-mutated colorectal cancer cell line. *Can J Physiol Pharmacol* **2021**, *99*, 284-293, doi: 10.1139/cjpp-2020-0449.
49. Ghavami, S.; Sharma, P.; Yeganeh, B.; Ojo, O.O.; Jha, A.; Mutawe, M.M.; Kashani, H.H.; Los, M.J.; Klonisch, T.; Unruh, H.; et al. Airway mesenchymal cell death by mevalonate cascade inhibition: integration of autophagy, unfolded protein

response and apoptosis focusing on Bcl2 family proteins. *Biochim Biophys Acta* **2014**, *1843*, 1259-1271, doi:10.1016/j.bbamcr.2014.03.006.
50. Hinton, M.; Eltayeb, E.; Ghavami, S.; Dakshinamurti, S. Effect of pulsatile stretch on unfolded protein response in a new model of the pulmonary hypertensive vascular wall. *Biochem Biophys Rep* **2021**, *27*, 101080, doi:10.1016/j.bbrep.2021.101080.
51. Alizadeh, J.; Kochan, M.M.; Stewart, V.D.; Drewnik, D.A.; Hannila, S.S.; Ghavami, S. Inhibition of Autophagy Flux Promotes Secretion of Chondroitin Sulfate Proteoglycans in Primary Rat Astrocytes. *Mol Neurobiol* **2021**, *58*, 6077-6091, doi: 10.1007/s12035-021-02533-4.
52. Ghavami, S.; Mutawe, M.M.; Schaafsma, D.; Yeganeh, B.; Unruh, H.; Klonisch, T.; Halayko, A.J. Geranylgeranyl transferase 1 modulates autophagy and apoptosis in human airway smooth muscle. *Am J Physiol Lung Cell Mol Physiol* **2012**, *302*, 420-428, doi: 10.1152/ajplung.00312.2011.
53. Ghavami, S.; Cunnington, R.H.; Yeganeh, B.; Davies, J.J.; Rattan, S.G.; Bathe, K.; Kavosh, M.; Los, M.J.; Freed, D.H.; Klonisch, T.; et al. Autophagy regulates trans fatty acid-mediated apoptosis in primary cardiac myofibroblasts. *Biochim Biophys Acta* **2012**, *1823*, 2274-2286, doi:10.1016/j.bbamcr.2012.09.008.
54. Klionsky, D.J.; Abdel-Aziz, A.K.; Abdelfatah, S.; Abdellatif, M.; Abdoli, A.; Abel, S.; Abeliovich, H.; Abildgaard, M.H.; Abudu, Y.P.; Acevedo-Arozena, A. Guidelines for the use and interpretation of assays for monitoring autophagy. *Autophagy* **2021**, *17*, 1-382, doi: 10.1080/15548627.2020.1797280.
55. Dastghaib, S.; Shojaei, S.; Mostafavi-Pour, Z.; Sharma, P.; Patterson, J.B.; Samali, A.; Mokarram, P.; Ghavami, S. Simvastatin induces unfolded protein response and enhances temozolomide-induced cell death in glioblastoma cells. *Cells* **2020**, *9*, 2339, doi: 10.3390/cells9112339.
56. Wang, Q.; Wang, J.; Wang, J.; Ju, X.; Zhang, H. Molecular mechanism of shikonin inhibiting tumor growth and potential application in cancer treatment. *Toxicol Res* **2021**, *10*, 1077-1084, doi: 10.1093/toxres/tfab107.
57. Shahsavari, Z.; Karami-Tehrani, F.; Salami, S. Shikonin induced necroptosis via reactive oxygen species in the T-47D breast cancer cell line. *Asian Pac J Cancer Prev* **2015**, *16*, 7261-7266, doi: 10.7314/apjcp.2015.16.16.7261.
58. Ma, X.; Yu, M.; Hao, C.; Yang, W. Shikonin induces tumor apoptosis in glioma cells via endoplasmic reticulum stress, and Bax/Bak mediated mitochondrial outer membrane permeability. *J Ethnopharmacol* **2020**, *263*, 113059, doi:10.1016/j.jep.2020.113059.
59. Paskeh, M.D.A.; Entezari, M.; Clark, C.; Zabolian, A.; Ranjbar, E.; Farahani, M.V.; Saleki, H.; Sharifzadeh, S.O.; Far, F.B.; Ashrafizadeh, M.; et al. Targeted regulation of autophagy using nanoparticles: New insight into cancer therapy. *Biochim Biophys Acta Mol Basis Dis* **2022**, *1868*, 166326, doi:10.1016/j.bbadis.2021.166326.
60. Yeganeh, B.; Rezaei Moghadam, A.; Alizadeh, J.; Wiechec, E.; Alavian, S.M.; Hashemi, M.; Geramizadeh, B.; Samali, A.; Bagheri Lankarani, K.; Post, M.; et al. Hepatitis B and C virus-induced hepatitis: Apoptosis, autophagy, and unfolded protein response. *World J Gastroenterol* **2015**, *21*, 13225-13239, doi:10.3748/wjg.v21.i47.13225.
61. Moosavi, M.A.; Sharifi, M.; Ghafary, S.M.; Mohammadalipour, Z.; Khataee, A.; Rahmati, M.; Hajjaran, S.; Los, M.J.; Klonisch, T.; Ghavami, S. Photodynamic N-TiO(2) Nanoparticle Treatment Induces Controlled ROS-mediated Autophagy and Terminal Differentiation of Leukemia Cells. *Sci Rep* **2016**, *6*, 34413, doi: 10.1038/srep34413.
62. Ghavami, S.; Eshragi, M.; Ande, S.R.; Chazin, W.J.; Klonisch, T.; Halayko, A.J.; McNeill, K.D.; Hashemi, M.; Kerkhoff, C.; Los, M. S100A8/A9 induces autophagy and apoptosis via ROS-mediated cross-talk between mitochondria and lysosomes that involves BNIP3. *Cell Res* **2010**, *20*, 314-331, doi:10.1038/cr.2009.129.
63. da Silva Rosa, S.C.; Martens, M.D.; Field, J.T.; Nguyen, L.; Kereliuk, S.M.; Hai, Y.; Chapman, D.; Diehl-Jones, W.; Aliani, M.; West, A.R.; et al. BNIP3L/Nix-induced mitochondrial fission, mitophagy, and impaired myocyte glucose uptake are abrogated by PRKA/PKA phosphorylation. *Autophagy* **2021**, *17*, 2257-2272, doi:10.1080/15548627.2020.1821548.
64. Chaabane, W.; Cieslar-Pobuda, A.; El-Gazzah, M.; Jain, M.V.; Rzeszowska-Wolny, J.; Rafat, M.; Stetefeld, J.; Ghavami, S.; Los, M.J. Human-gyrovirus-Apoptin triggers mitochondrial death pathway--Nur77 is required for apoptosis triggering. *Neoplasia* **2014**, *16*, 679-693, doi:10.1016/j.neo.2014.08.001.
65. Ghavami, S.; Eshragi, M.; Ande, S.R.; Chazin, W.J.; Klonisch, T.; Halayko, A.J.; Mcneill, K.D.; Hashemi, M.; Kerkhoff, C.; Los, M. S100A8/A9 induces autophagy and apoptosis via ROS-mediated cross-talk between mitochondria and lysosomes that involves BNIP3. *Cell Res* **2010**, *20*, 314-331, doi: 10.1038/cr.2009.129.
66. Ghavami, S.; Mutawe, M.M.; Schaafsma, D.; Yeganeh, B.; Unruh, H.; Klonisch, T.; Halayko, A.J. Geranylgeranyl transferase 1 modulates autophagy and apoptosis in human airway smooth muscle. *Am J Physiol Lung Cell Mol Physiol* **2012**, *302*, 420-428, doi: 10.1152/ajplung.00312.2011.
67. Rashid, M.U.; Lorzadeh, S.; Gao, A.; Ghavami, S.; Coombs, K.M. PSMA2 knockdown impacts expression of proteins involved in immune and cellular stress responses in human lung cells. *Biochim Biophys Acta Mol Basis Dis* **2022**, *1869*, 166617, doi:10.1016/j.bbadis.2022.166617.
68. Sharma, P.; McAlinden, K.D.; Ghavami, S.; Deshpande, D.A. Chloroquine: Autophagy inhibitor, antimalarial, bitter taste receptor agonist in fight against COVID-19, a reality check? *Eur J Pharmacol* **2021**, *897*, 173928, doi:10.1016/j.ejphar.2021.173928.
69. Gupta, S.S.; Zeglinski, M.R.; Rattan, S.G.; Landry, N.M.; Ghavami, S.; Wigle, J.T.; Klonisch, T.; Halayko, A.J.; Dixon, I.M. Inhibition of autophagy inhibits the conversion of cardiac fibroblasts to cardiac myofibroblasts. *Oncotarget* **2016**, *7*, 78516-78531, doi:10.18632/oncotarget.12392.

70. Ghavami, S.; Mutawe, M.M.; Hauff, K.; Stelmack, G.L.; Schaafsma, D.; Sharma, P.; McNeill, K.D.; Hynes, T.S.; Kung, S.K.; Unruh, H.; et al. Statin-triggered cell death in primary human lung mesenchymal cells involves p53-PUMA and release of Smac and Omi but not cytochrome c. *Biochim Biophys Acta* **2010**, *1803*, 452-467, doi:10.1016/j.bbamcr.2009.12.005.
71. Ghavami, S.; Mutawe, M.M.; Sharma, P.; Yeganeh, B.; McNeill, K.D.; Klonisch, T.; Unruh, H.; Kashani, H.H.; Schaafsma, D.; Los, M.; et al. Mevalonate cascade regulation of airway mesenchymal cell autophagy and apoptosis: a dual role for p53. *PLoS One* **2011**, *6*, e16523, doi:10.1371/journal.pone.0016523.
72. Barzegar Behrooz, A.; Talaie, Z.; Jusheghani, F.; Los, M.J.; Klonisch, T.; Ghavami, S. Wnt and PI3K/Akt/mTOR Survival Pathways as Therapeutic Targets in Glioblastoma. *Int J Mol Sci* **2022**, *23*, 1353, doi: 10.3390/ijms23031353.
73. Fekrirad, Z.; Barzegar Behrooz, A.; Ghaemi, S.; Khosrojerdi, A.; Zarepour, A.; Zarrabi, A.; Arefian, E.; Ghavami, S. Immunology Meets Bioengineering: Improving the Effectiveness of Glioblastoma Immunotherapy. *Cancers (Basel)* **2022**, *14*, 3698, doi: 10.3390/cancers14153698.
74. Nakada, M.; Furuta, T.; Hayashi, Y.; Minamoto, T.; Hamada, J.-i. The strategy for enhancing temozolomide against malignant glioma. *Front Oncol* **2012**, *2*, 98, doi: 10.3389/fonc.2012.00098.
75. Nielsen, S.F.; Nordestgaard, B.G.; Bojesen, S.E. Statin use and reduced cancer-related mortality. *N Engl J Med* **2013**, *368*, 576-577, doi: 10.1056/NEJMc1214827.
76. Gaist, D.; Hallas, J.; Friis, S.; Hansen, S.; Sørensen, H.T. Statin use and survival following glioblastoma multiforme. *Cancer Epidemiol* **2014**, *38*, 722-727, doi: 10.1016/j.canep.2014.09.010.
77. Farwell, W.R.; Scranton, R.E.; Lawler, E.V.; Lew, R.A.; Brophy, M.T.; Fiore, L.D.; Gaziano, J.M. The association between statins and cancer incidence in a veterans population. *J Natl Cancer Inst* **2008**, *100*, 134-139, doi: 10.1093/jnci/djm286.
78. Yeganeh, B.; Wiechec, E.; Ande, S.R.; Sharma, P.; Moghadam, A.R.; Post, M.; Freed, D.H.; Hashemi, M.; Shojaei, S.; Zeki, A.A. Targeting the mevalonate cascade as a new therapeutic approach in heart disease, cancer and pulmonary disease. *Pharmacol Ther* **2014**, *143*, 87-110, doi: 10.1016/j.pharmthera.2014.02.007.
79. Zhu, Z.; Zhang, P.; Li, N.; Kiang, K.M.Y.; Cheng, S.Y.; Wong, V.K.-W.; Leung, G.K.-K. Lovastatin enhances cytotoxicity of temozolomide via impairing autophagic flux in glioblastoma cells. *Biomed Res Int* **2019**, *2019*, 2710693, doi: 10.1155/2019/2710693.
80. Palko-Łabuz, A.; Środa-Pomianek, K.; Wesołowska, O.; Kostrzewa-Susłow, E.; Uryga, A.; Michalak, K. MDR reversal and pro-apoptotic effects of statins and statins combined with flavonoids in colon cancer cells. *Biomed Pharmacother* **2019**, *109*, 1511-1522, doi: 10.1016/j.biopha.2018.10.169.
81. Luput, L.; Sesarman, A.; Porfire, A.; Achim, M.; Muntean, D.; Casian, T.; Patras, L.; Rauca, V.F.; Drotar, D.M.; Stejerean, I. Liposomal simvastatin sensitizes C26 murine colon carcinoma to the antitumor effects of liposomal 5-fluorouracil in vivo. *Cancer Sci* **2020**, *111*, 1344-1356, doi: 10.1111/cas.14312.
82. Hwang, K.-E.; Park, C.; Kwon, S.-J.; Kim, Y.-S.; Park, D.-S.; Lee, M.-K.; Kim, B.-R.; Park, S.-H.; Yoon, K.-H.; Jeong, E.-T. Synergistic induction of apoptosis by sulindac and simvastatin in A549 human lung cancer cells via reactive oxygen species-dependent mitochondrial dysfunction. *Int J Oncol* **2013**, *43*, 262-270, doi: 10.3892/ijo.2013.1933.
83. Hwang, K.-E.; Kim, Y.-S.; Hwang, Y.-R.; Kwon, S.-J.; Park, D.-S.; Cha, B.-K.; Kim, B.-R.; Yoon, K.-H.; Jeong, E.-T.; Kim, H.-R. Enhanced apoptosis by pemetrexed and simvastatin in malignant mesothelioma and lung cancer cells by reactive oxygen species-dependent mitochondrial dysfunction and Bim induction. *Int J Oncol* **2014**, *45*, 1769-1777, doi: 10.3892/ijo.2014.2584.
84. Alizadeh, J.; Zeki, A.A.; Mirzaei, N.; Tewary, S.; Rezaei Moghadam, A.; Glogowska, A.; Nagakannan, P.; Eftekharpour, E.; Wiechec, E.; Gordon, J.W. Mevalonate cascade inhibition by simvastatin induces the intrinsic apoptosis pathway via depletion of isoprenoids in tumor cells. *Sci Rep* **2017**, *7*, 1-14, doi: 10.1038/srep44841.
85. Cha, H.S.; Lee, H.K.; Park, S.H.; Nam, M.J. Acetylshikonin induces apoptosis of human osteosarcoma U2OS cells by triggering ROS-dependent multiple signal pathways. *Toxicol in Vitro* **2023**, *86*, 105521, doi:10.1016/j.tiv.2022.105521.
86. Lim, H.M.; Lee, J.; Yu, S.H.; Nam, M.J.; Cha, H.S.; Park, K.; Yang, Y.H.; Jang, K.Y.; Park, S.H. Acetylshikonin, A Novel CYP2J2 Inhibitor, Induces Apoptosis in RCC Cells via FOXO3 Activation and ROS Elevation. *Oxid Med Cell Longev* **2022**, *2022*, 9139338, doi:10.1155/2022/9139338.
87. Lim, H.M.; Lee, J.; Nam, M.J.; Park, S.-H. Acetylshikonin induces apoptosis in human colorectal cancer HCT-15 and LoVo cells via nuclear translocation of FOXO3 and ROS level elevation. *Oxid Med Cell Longev* **2021**, *2021*, 6647107, doi: 10.1155/2021/6647107.
88. Lohberger, B.; Glanzer, D.; Kaltenegger, H.; Eck, N.; Leithner, A.; Bauer, R.; Kretschmer, N.; Steinecker-Frohnwieser, B. Shikonin derivatives cause apoptosis and cell cycle arrest in human chondrosarcoma cells via death receptors and MAPK regulation. *BMC Cancer* **2022**, *22*, 758, doi: 10.1186/s12885-022-09857-x.
89. Hao, G.; Zhai, J.; Jiang, H.; Zhang, Y.; Wu, M.; Qiu, Y.; Fan, C.; Yu, L.; Bai, S.; Sun, L.; et al. Acetylshikonin induces apoptosis of human leukemia cell line K562 by inducing S phase cell cycle arrest, modulating ROS accumulation, depleting Bcr-Abl and blocking NF-kappaB signaling. *Biomed Pharmacother* **2020**, *122*, 109677, doi:10.1016/j.biopha.2019.109677.
90. Zhao, Q.; Kretschmer, N.; Bauer, R.; Efferth, T. Shikonin and its derivatives inhibit the epidermal growth factor receptor signaling and synergistically kill glioblastoma cells in combination with erlotinib. *Int J Cancer* **2015**, *137*, 1446-1456, doi: 10.1002/ijc.29483.
91. Wang, X.; Welsh, N. Bcl-2 maintains the mitochondrial membrane potential, but fails to affect production of reactive oxygen species and endoplasmic reticulum stress, in sodium palmitate-induced beta-cell death. *Ups J Med Sci* **2014**, *119*, 306-315, doi:10.3109/03009734.2014.962714.

92. Hawkins, B.J.; Levin, M.D.; Doonan, P.J.; Petrenko, N.B.; Davis, C.W.; Patel, V.V.; Madesh, M. Mitochondrial complex II prevents hypoxic but not calcium- and proapoptotic Bcl-2 protein-induced mitochondrial membrane potential loss. *J Biol Chem* **2010**, *285*, 26494-26505, doi:10.1074/jbc.M110.143164.
93. Schimmer, A.D.; Hedley, D.W.; Pham, N.A.; Chow, S.; Minden, M.D. BAD induces apoptosis in cells over-expressing Bcl-2 or Bcl-xL without loss of mitochondrial membrane potential. *Leuk Lymphoma* **2001**, *42*, 429-443, doi: 10.3109/10428190109064600.
94. Ghavami, S.; Yeganeh, B.; Stelmack, G.L.; Kashani, H.H.; Sharma, P.; Cunnington, R.; Rattan, S.; Bathe, K.; Klonisch, T.; Dixon, I.M.; et al. Apoptosis, autophagy and ER stress in mevalonate cascade inhibition-induced cell death of human atrial fibroblasts. *Cell Death Dis* **2012**, *3*, e330, doi:10.1038/cddis.2012.61.
95. Wu, M.D.; Zhang, Y.Y.; Yi, S.Y.; Sun, B.B.; Lan, J.; Jiang, H.M.; Hao, G.P. Acetylshikonin induces autophagy-dependent apoptosis through the key LKB1-AMPK and PI3K/Akt-regulated mTOR signalling pathways in HL-60 cells. *J Cell Mol Med* **2022**, *26*, 1606-1620, doi:10.1111/jcmm.17202.
96. Moon, J.; Koh, S.S.; Malilas, W.; Cho, I.R.; Kaewpiboon, C.; Kaowinn, S.; Lee, K.; Jhun, B.H.; Choi, Y.W.; Chung, Y.H. Acetylshikonin induces apoptosis of hepatitis B virus X protein-expressing human hepatocellular carcinoma cells via endoplasmic reticulum stress. *Eur J Pharmacol* **2014**, *735*, 132-140, doi:10.1016/j.ejphar.2014.04.021.
97. Ahmadi, M.; Madrakian, T.; Ghavami, S. Preparation and Characterization of Simvastatin Nanocapsules: Encapsulation of Hydrophobic Drugs in Calcium Alginate. *Methods Mol Biol* **2020**, *2125*, 47-56, doi: 10.1007/7651_2018_191.
98. Yang, J.; Liu, X.; Bhalla, K.; Kim, C.N.; Ibrado, A.M.; Cai, J.; Peng, T.-I.; Jones, D.P.; Wang, X. Prevention of apoptosis by Bcl-2: release of cytochrome c from mitochondria blocked. *Science* **1997**, *275*, 1129-1132, doi : 10.1126/science.275.5303.1129.